

GROUND MOTION AND ITS EFFECTS IN ACCELERATOR DESIGN*

G. E. Fischer

Stanford Linear Accelerator Center, Stanford University, Stanford, CA 94305

TABLE OF CONTENTS

		Page
1	Introduction	3
	1.1 Why is Ground Motion an Issue?	3
	1.2 Some Possibly Serious Consequences of Ground Motion	6
	1.3 What Are We Left With After Counter Measures Are Taken?	6
2	Types of Motion	7
	2.1 Ground Settlement	8
	2.2 Earth Tides and Free Oscillations	12
	2.3 Seismic Disturbances	12
	2.3.1 Earthquakes	12
	2.3.2 Natural Microseismic Noise	18
3	A Digression	21
	3.1 How Does Sound Propagate in an Elastic Medium?	21
	3.2 Properties of the Fourier Transform	27
4	Frequencies of Interest	37
5	Some Measurements at SLAC	42
	5.1 Instrumentation	42
	5.1.1 Sensors	42
	5.1.2 Data Display and Recording	42
	5.2 Data	42
	5.2.1 Base Levels	42
	5.2.2 Transient Disturbances	48

* Work supported by the Department of Energy, contract DE-AC03-76SF00515.

Invited talk presented at the 1984 Summer School on High Energy
Particle Accelerators, Batavia, Illinois, August 13-24, 1984

5.2.3	Traffic	57
5.2.4	Continuously Operating Machines	57
5.2.5	Detector Assembly Activity	57
5.2.6	Relative Phase Measurements	58
6	Some General Comments Regarding Local Sources	62
6.1	Geometric Spreading	62
6.2	Attenuation within the Medium (Inelasticity)	62
6.3	More on Velocities in the Ground	65
7	What To Do About the Problem?	70
7.1	Natural Site Considerations	70
7.2	Mitigation of Sources	70
7.3	Component and Component Support Design	70
7.3.1	Theoretical Analysis	72
7.3.2	Experimental Analysis	72
7.4	Feedback on Beam Derived Information	74
7.5	Feedback/Feedforward on Seismic Array Derived Information	75
8	Summary	75
9	References	76

GROUND MOTION AND ITS EFFECTS IN ACCELERATOR DESIGN

G. E. Fischer

Stanford Linear Accelerator Center, Stanford University, Stanford, CA 94305

1. INTRODUCTION

It may strike students of accelerator physics as somewhat bizarre that the topic of *ground motion* (normally left to the practitioners of civil engineering and mechanical alignment) should find its way, this year, into a course of summer school lectures. The reason for this is, I believe, that in some large future machine, ground motion effects, if not ameliorated, will present fundamental limitations in accelerator performance. With respect to linear colliders, we are nearing this time today.

In this hour we must touch on many aspects of the earth sciences, disciplines I have only recently become acquainted with. The presentation will be only partially analytic and mostly anecdotal. It used to be said that when embarking on a project, the first thing one had to do was to hire a good lawyer to keep one out of trouble. I think this maxim should now be extended to include a geophysicist. Be that as it may, the extensive references listed at the end should at least steer you in the direction of this body of knowledge.

1.1 WHY IS GROUND MOTION AN ISSUE?

With the introduction of strong focussing to contain transverse phase space (thereby reducing the cost of magnets) in the past 30 years apertures have been reduced from meters (Bevatron) to a few tens of centimeters. As energies continue to climb, modern machines will have apertures of a few centimeters or even less. The alignment of strong focussing elements has therefore become ever more critical. In addition, the recognition that the beam's wake-fields interact with the walls of the vacuum chamber or accelerator structure leads to stringent positional tolerances on beam centering.

More quantitatively let us consider some general lattice of magnetic elements for a circular machine as shown in Fig. 1.1.

Question: What happens to the beam if we displace some flat field bending magnet in the x direction?

Answer: To first order - nothing!

Q: What happens if we move a single quadrupole an amount d in the y direction at location (1)?

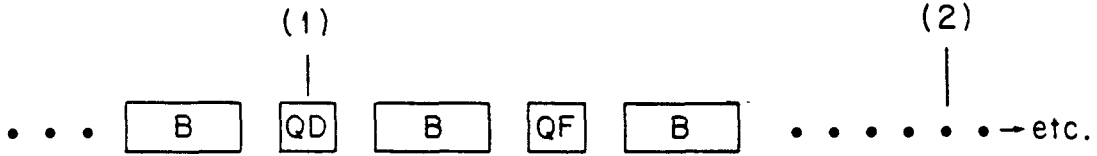


Fig. 1.1. A General Machine Lattice.

A: We have introduced an *error dipole field* that kicks the beam through an angle θ .

Q: What is the magnitude of the resulting orbit distortion at say point (2)?

A:

$$\delta y_{(2)} = \frac{\theta_{(1)} \sqrt{(\beta_1 \beta_2)}}{2 \sin \pi \nu} \cos(\phi_2 - \phi_1 - \pi \nu)$$

in which $\theta = gl\delta_y/Br$ where $g = \text{gradient}$,

$l = \text{quad length}$,

$\delta_y = \text{displacement}$.

Note the *resonant* term $\sin \pi \nu$ in the denominator in which ν is the betatron frequency.

Let us now assume that all the defocussing quads in N lattice cells are displaced in some *statistically random* manner in amplitude and direction of transverse displacement and sum up their contributions. The above expression is replaced by:

$$\delta y_{2 \text{ rms}} = \frac{\langle \delta_Q \text{ rms} \rangle \sqrt{(\beta_y \text{ quads } \beta_{(2)})} \sqrt{N}}{2\sqrt{2} |\sin \pi \nu|} gl/Br$$

Q: For example, what is the rms displacement of the beam at the interaction point (IP) of, say, the "SSC" if we let the lattice quads in this machine *jiggle* randomly by 1 micron (10^{-6} meters)?

CAUTION: I am *not* suggesting that all quads be initially aligned to this accuracy – a clearly impossible task! We assume that some extensive system of beam position monitors and DC correcting coils has already been employed to center the beam in the vacuum chamber. The 1 micron referred to here is the jittering (time dependent) magnet motion.

A: Inserting some representative SSC parameters at 20 TeV,¹

$$\beta_{\text{quads}} = 276 \text{ meters}, \quad g = 200 \text{ T/m}, \quad l_{\text{quad}} = 4.25 \text{ m},$$

$$\beta_y \text{ at the I.P.} = 2 \text{ m}, \quad B\rho = 66735 \text{ T-m},$$

$$N = 516, \quad \nu = 97.25 \quad \delta_q \text{ rms} = 1.0 \times 10^{-6} \text{ m},$$

one obtains $\langle y_{IP} \rangle \text{ rms} = \delta_Q \times 3.4 = 3.4 \text{ microns rms}$

Q: Is this serious?

A: Potentially yes, because the vertical beam size (σ_y) of the SSC beam at the I.P. is about 9 microns. Loss of luminosity would occur, but, far more importantly, the non-linear beam-beam interaction would become asymmetric.

Q: Is this example a realistic representation of the physical situation?

A: No, we will see that quads are not likely to move *randomly* by 1 micron. But, it was an easy calculation to do in order to give the reader a feeling for the magnitudes involved in the problem. Under certain conditions, the situation could be better or worse.

Shortly after this lecture was first given in the fall of 1984, P. Morton (SLAC) pointed out that in a "closed circle particle-antiparticle" collider (such as an e^+e^- or p^+p^- storage ring) both beams suffer the same equilibrium orbit distortion and would continue to collide properly unless the quadrupoles are moved on the time scale of a revolution period. Since mechanical objects cannot move at such frequencies effects of the kind alluded to would not be observed. The case of p^+p^+ is not clear at the moment since the orbits are not necessarily identical.

Another important point, the spatial coherence of quad motion was discussed in a very elegant paper in January 1985 by T. Aniel and J.L. Laclare.²⁸ In their analysis they calculate the response of a beam to randomly oriented plane wave disturbances passing through the site and not surprisingly find that a uniform ring structure picks out the betatron wavelength. The analysis is valid under the assumption that the motion of the quadrupoles follows that of the ground completely.

Exercise 1: Calculate the relative displacements of two linear collider beams at the I.P. if the final interaction region quad packages move transversely in opposite directions by 1 micron.

1.2 SOME POSSIBLY SERIOUS CONSEQUENCES OF GROUND MOTION

The following is a partial list of effects one can conjure up that may occur due to ground displacement of elements. The list is clearly not meant to be complete, nor have the magnitudes of the effects on machine performance been evaluated in each case in detail. The purpose of this lecture is only to "alert" the reader and to then describe what is known about the motion itself.

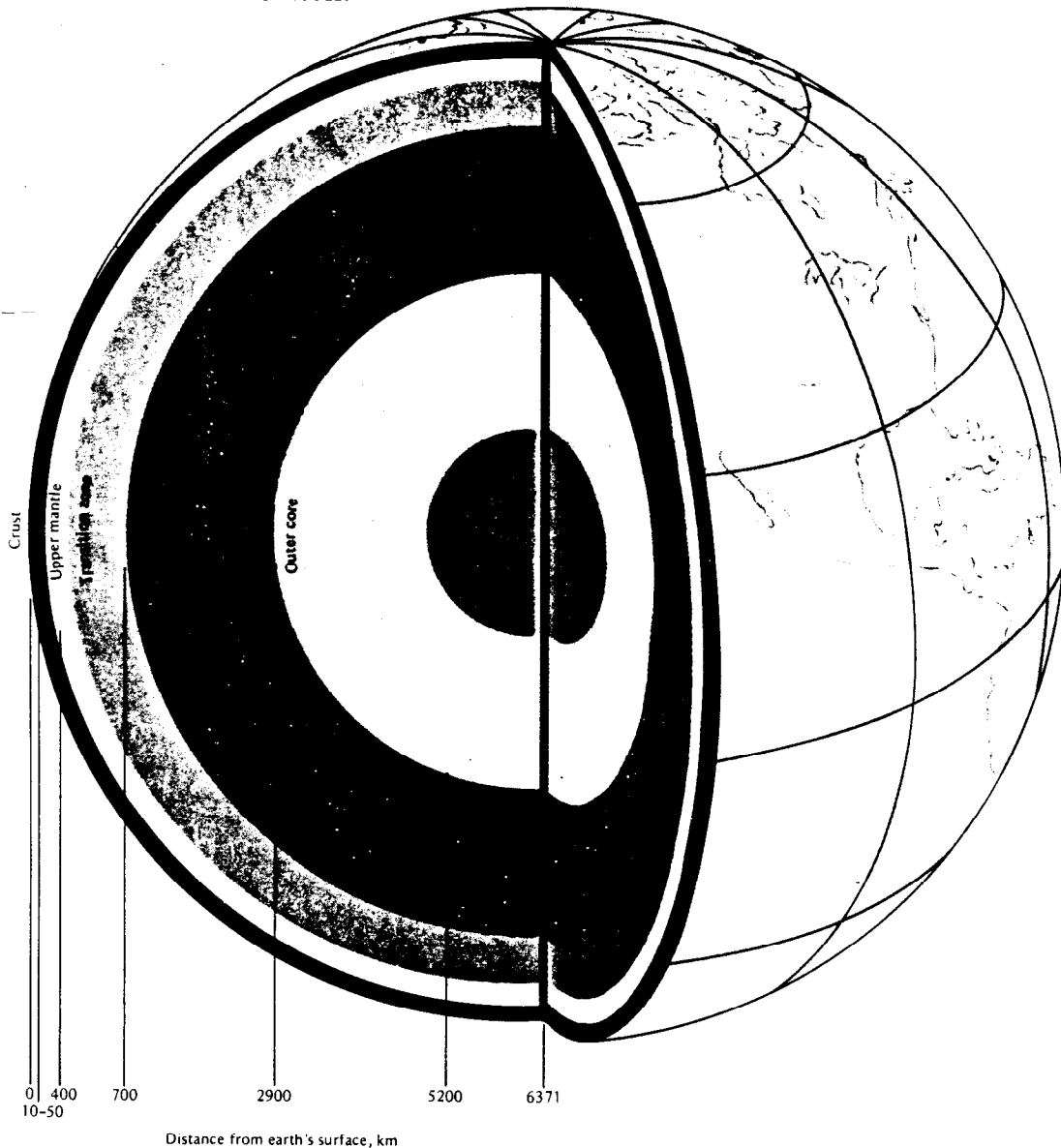
1. We have already alluded to the problem of off-axis beam collisions in an SSC – a proton collider having little natural, if any, damping to restore possible transverse phase space dilution.
2. Distorted orbits have slightly different path lengths so that random arrival times of the bunch at the r-f accelerating cavities will appear as a source of phase noise possibly causing longitudinal phase space dilution with its own consequences.
3. Large betatron oscillations of the beam in sextupolar fields (present in all modern machines to correct chromaticities) give rise to phase space tumbling or filamentation (dilution) with resulting loss of luminosity. This is particularly true in the arc transport system of the SLC presently under construction.
4. The positional jitter tolerances on the SLC arc magnets are in fact about 0.1 microns because the beam at the I.P. is about 1.5 microns in size.
5. Interaction region quads, by virtue of the beams' very large beta values therein, are generally very sensitive elements.
6. We have already noted the denominator in the orbit distortion formula. In a circular machine we must, of course, avoid integer (and certain higher) resonances. It is possible, however, to imagine situations in which the motion of focussing elements is such that errors occur "in tune" with the particles' motion over a single pass or revolution.
7. Last, but not least, in particular in a linear collider, wakefield effects are driven by orbit distortions. This sets a tolerance of about 0.7μ rms for the linac quads at SLC and about 0.05μ rms for a super linear collider.²

1.3 WHAT ARE WE LEFT WITH AFTER COUNTER MEASURES ARE TAKEN?

Feedback, and in some circumstances feedforward, is the panacea of the accelerator physicist after all sensible counter measures described below are applied. We will see that there are limitations. It is my unsubstantiated guess today that a machine that calls for positional tolerances less than, say, 0.005μ in the range 1 to 30 Hz will be extremely difficult to operate.

2. TYPES OF MOTION

When one considers the geophysical makeup of the planet Earth, one quickly realizes that terra firma will behave more like a bowl of jello covered by a rather thin, *elastic*, slightly wrinkly and broken skin. Figure 2.1³ shows that the crust is, in fact, only between 7.5 to 35 km thick. The upper mantle is gooey, and the so-called outer core must be quite liquid. In this section, we will discuss various types of motion in increasing range of frequency. For generality we list not only those relevant to our problem but also a few which can be dismissed from further consideration.



Regions of the earth's interior. The depth shown for the crust, 17 km, is the weighted average of oceanic crust (7.5 km) and continental crust (35 km).

Fig. 2.1. Crust and Interior of the Earth (from Ref. 3).

2.1 GROUND SETTLEMENT

Seasonal variations in the local ground water table, water content of the soil, further compaction of even well engineered fill or rebound of the ground under cuts etc., all tend to push the tunnel out of its original shape.

For example, the SLAC linac "cut and cover" tunnel is 10,000 feet long and has built into it a laser alignment system capable of a transverse resolution of about .001 inches.⁴ Figures 2.2(a,b), show the cumulative displacements of some 240 targets along the line, in the horizontal and vertical directions – summed over the 17 years 1966 to 1983. Although the motions were faster just after initial construction, recent yearly surveys still indicate motions in certain regions of the order 1/2 mm/year. Generally speaking, the wavelengths of the distortions are comparable or larger than the betatron wavelength of the focussing structure and, therefore, less dangerous. Needless to say, the accelerator waveguide is readjusted once a year.

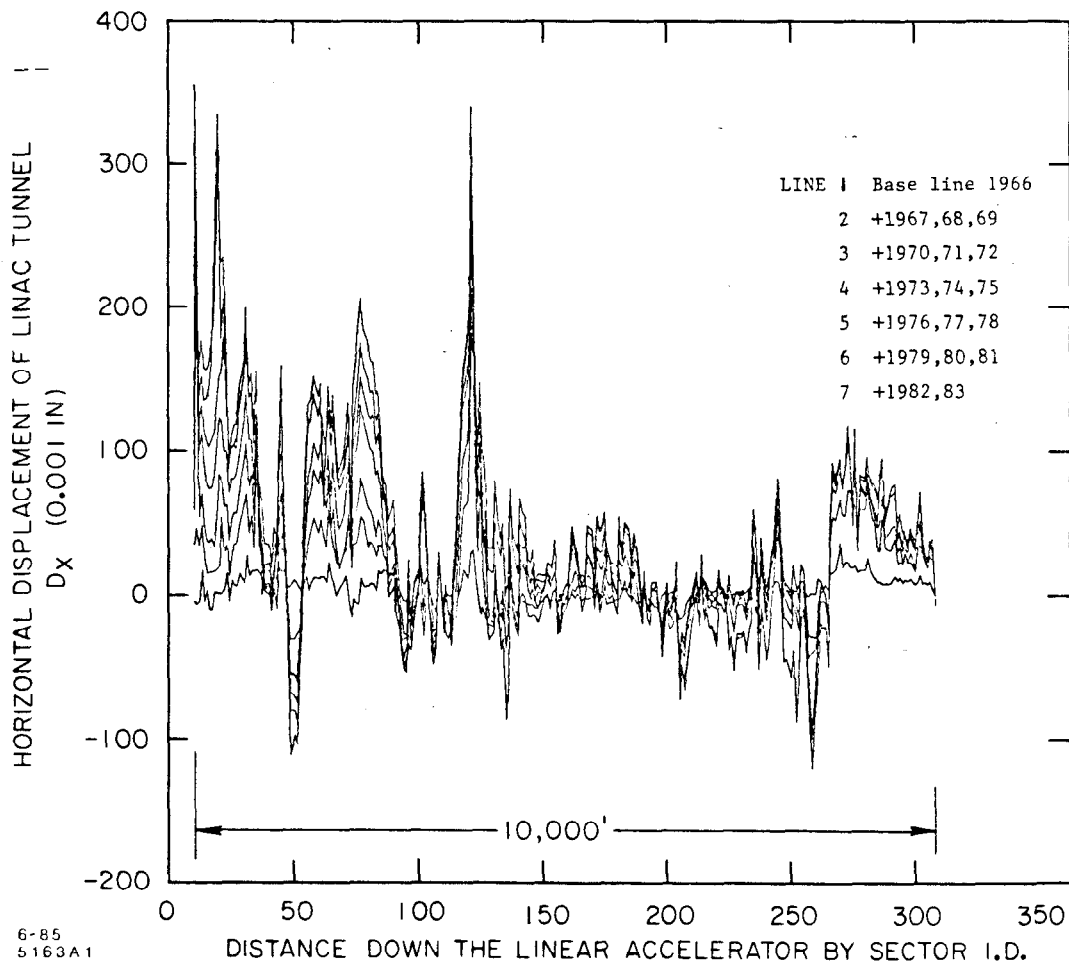


Fig. 2.2(a). Displacement of the SLAC Linac Tunnel – Horizontal.

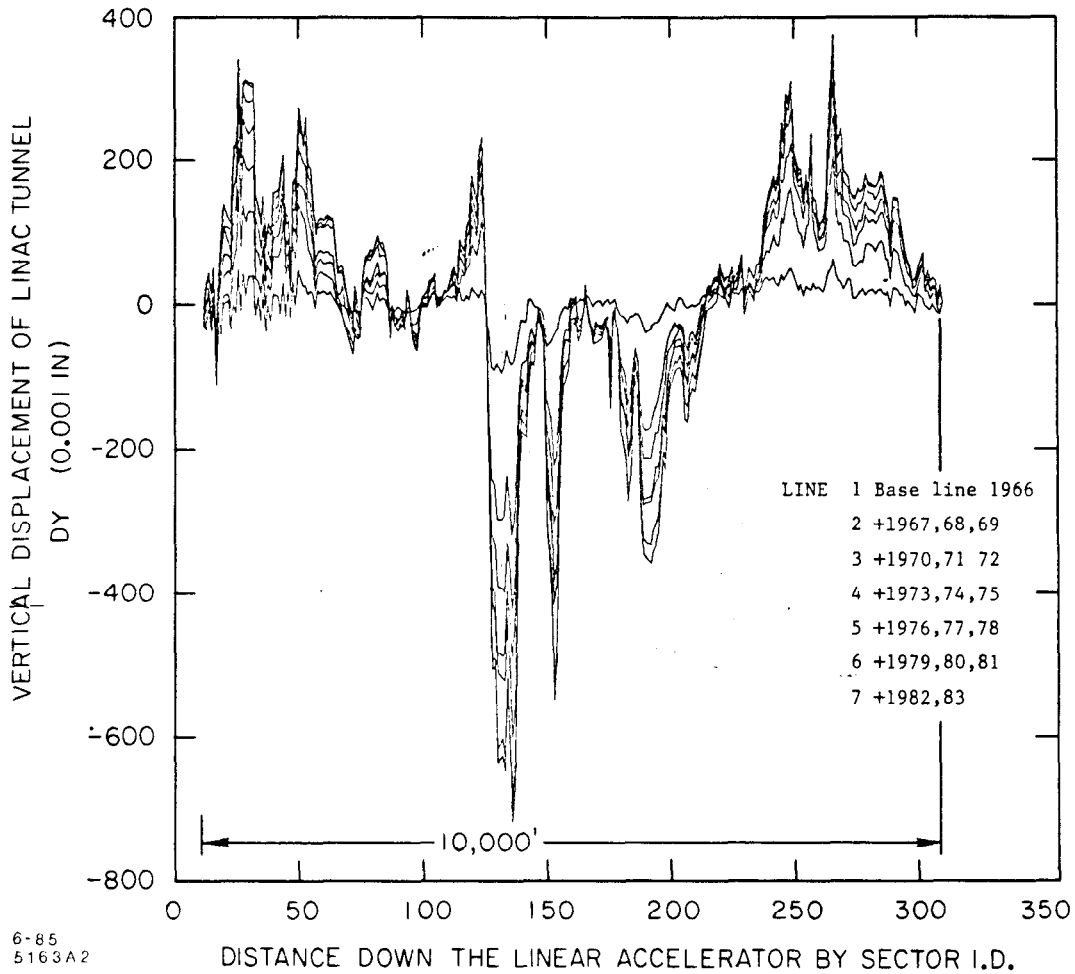
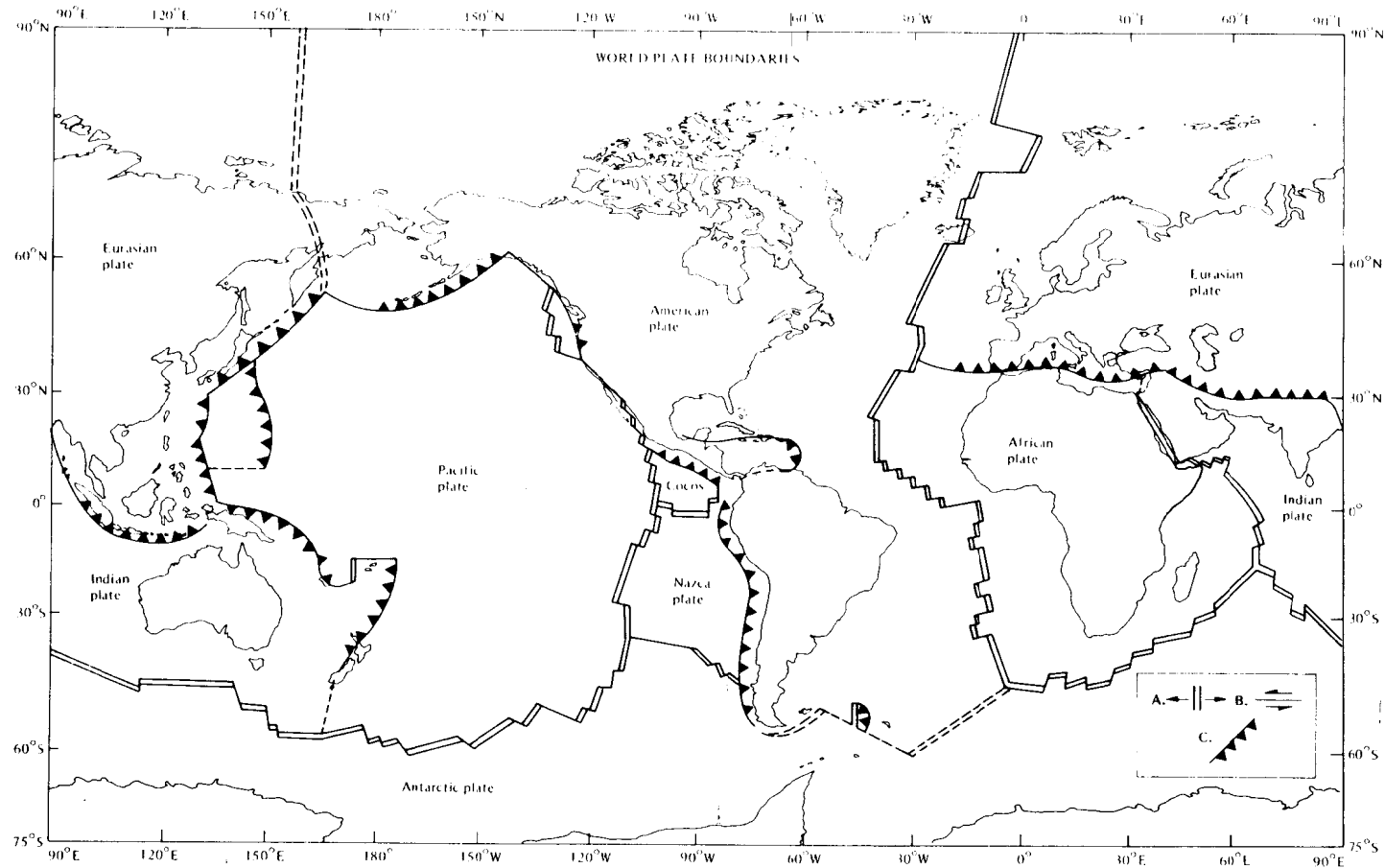


Fig. 2.2(b). Displacement of the SLAC Linac Tunnel - Vertical.

It was expected that, since the Pacific Tectonic Plate (see Fig. 2.3) is inexorably grinding northward (and in places downward) at the rate of about 2.6 inches/year, and since the San Andreas Fault is "locked" in northern California, that the tunnel would be eventually bent northward at the western end of the accelerator. Interestingly enough, the data does not exhibit this effect.



Major plates of the world. The types of plate boundaries, marked by heavy lines, are discussed later. A. Midoceanic ridges at which the plates move apart are represented by double lines. B. Transform fault boundaries are shown by single lines. C. Trenches and other subduction zones are marked by lines with teeth on one side. The teeth point down the descending slab. Dotted lines are used where the exact location or nature of the boundary is uncertain.

Fig. 2.3. Tectonic Plates of the Earth's Surface (from Ref. 3).

Another example from experience at SLAC concerns the behavior of the PEP tunnel. The diameter of this storage ring is 700 m. Vertical alignment is performed by means of a precise "*circumferentially continuous*" water level⁵. After initial settlement of about 3 mm in the first year, local vertical excursions are now less than 1/2 mm/year. Sharp local discontinuities (approximately 2 mm) occur only near experimental regions whenever large detectors, about 1000 tons, depress the hall floors. Curiously, since its construction, the ring as a whole appears to have tilted (down at the west) about 1/2 mm across its diameter. It may be well to point out that tunnels at SLAC, with a few notable exceptions sit on, or are mined in, grey, unweathered, well-cemented, tertiary myocene sandstone (age about 25 million years). The properties of this material are quite variable and are described later.

2.2 EARTH TIDES AND FREE OSCILLATIONS

Recognizing that the earth behaves as an *elastic* body at short time scales, it is not hard to believe that the time varying forces exerted by the moon and sun distort the gravitational potential not only of the surface water (which is free to slosh about in the ocean basin) but of the body as a whole. Diurnal (actually 24 hours 50 minutes) and semidiurnal amplitudes of the landmass result with amplitudes in the centimeter range,⁶ Berger and Lovberg 1970. Following shock excitation from large earthquakes, the planet can ring like a gong! Spheroidal and torsional modes have been seen with periods ranging from 50 minutes to a few minutes for the higher modes – an interesting type of *spectroscopy*. To the accelerator builder, however, these motions are nothing more than a curiosity, because over the dimensions of the site of even the most ambitious project, they will *not* cause relative quad displacements.

2.3 SEISMIC DISTURBANCES

2.3.1 Earthquakes

Although most of what is known about the earth's composition is derived from the seismologic study of these events, we will see below that they interest the accelerator designer mainly in the design of buildings and structures.

Most, but not all, earthquakes occur at the interface of moving tectonic plates. See Fig. 2.4. The dominant feature in California is the system of faults associated with the San Andreas. This fault and its tributaries are clearly visible in Fig. 2.5 on which are plotted, for example, all quakes in the area of the year 1978.⁷

The number of earthquakes N per unit time of magnitude greater than M may be written:

$$\log_{10} N = a - b M \quad \text{in which} \quad b \approx 1$$

and in which the constant a is characteristic of the geographical area covered and the density of detectors. For the Central California Microearthquake Network operated by the U.S.G.S. in Menlo Park covering 50,000 square miles with 250 stations (mostly along the San Andreas), some 4000 earthquakes are detected each year. In the 3 years 1976-1979, only 18 events of magnitude 1.5 to 3.5 occurred with epicenters within 20 km of the collider site.

The magnitude M of an earthquake is defined as the logarithm of some quantity related to amplitude, energy release, seismic moment, etc., of the event. Since statistically speaking small events happen frequently (large events seldom) one is led to the notion that if stress is building up linearly with time, and if the

World map of earthquake epicenters. The solid colored dots represent shallow earthquakes originating at depths of less than 70 km. The long linear belts of shallow earthquakes mark the boundaries of the plates. The light colored dots mark earthquakes with focal depths between 70 and 300 km. The black dots represent earthquakes whose foci lay deeper than 300 km. Most of these deeper earthquakes occur within a down-going plate rather than on a boundary between plates. [Data from Environmental Science Services Administration (ESSA).]

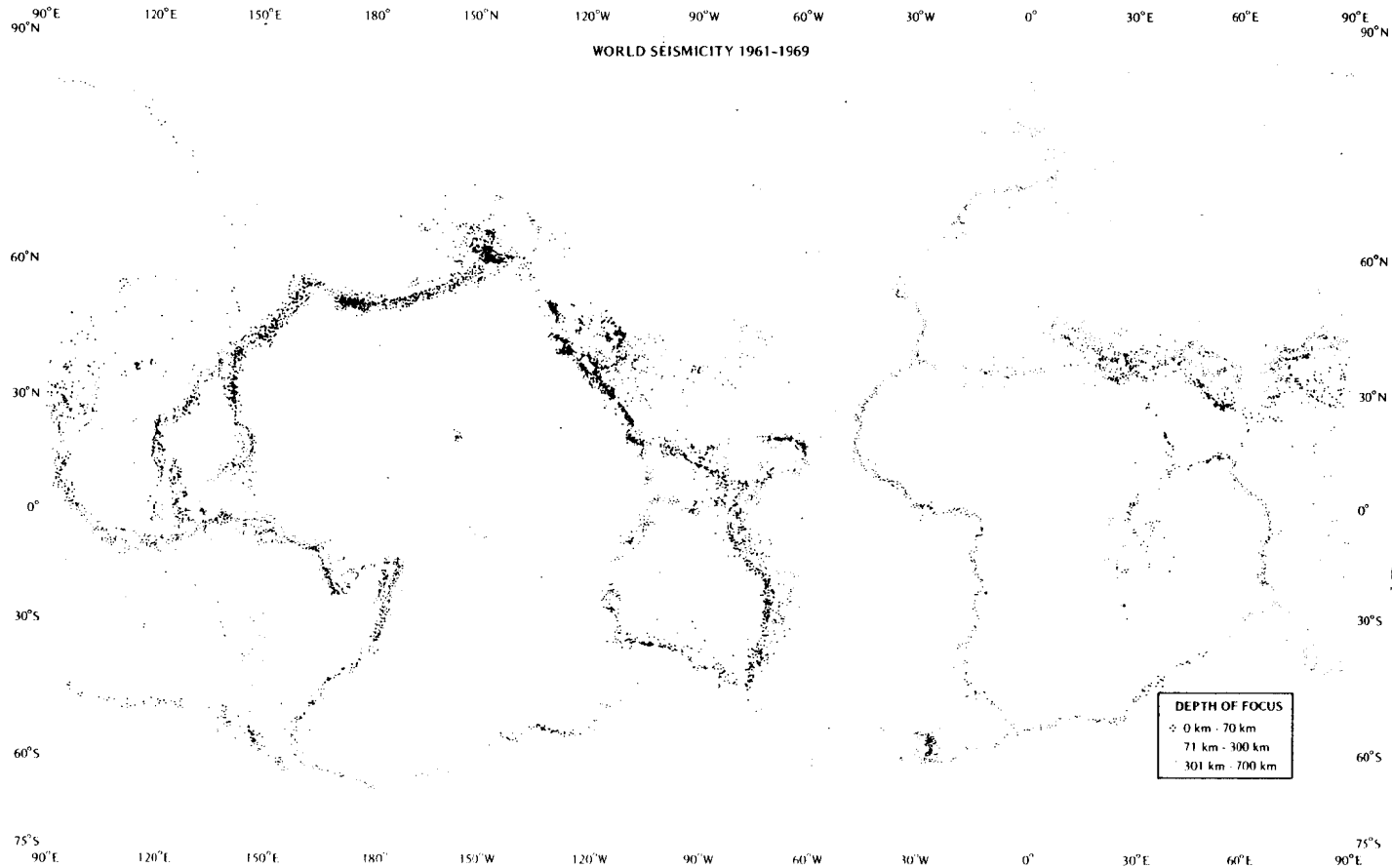


Fig. 2.4. Major Earthquakes in the World (from Ref. 3).

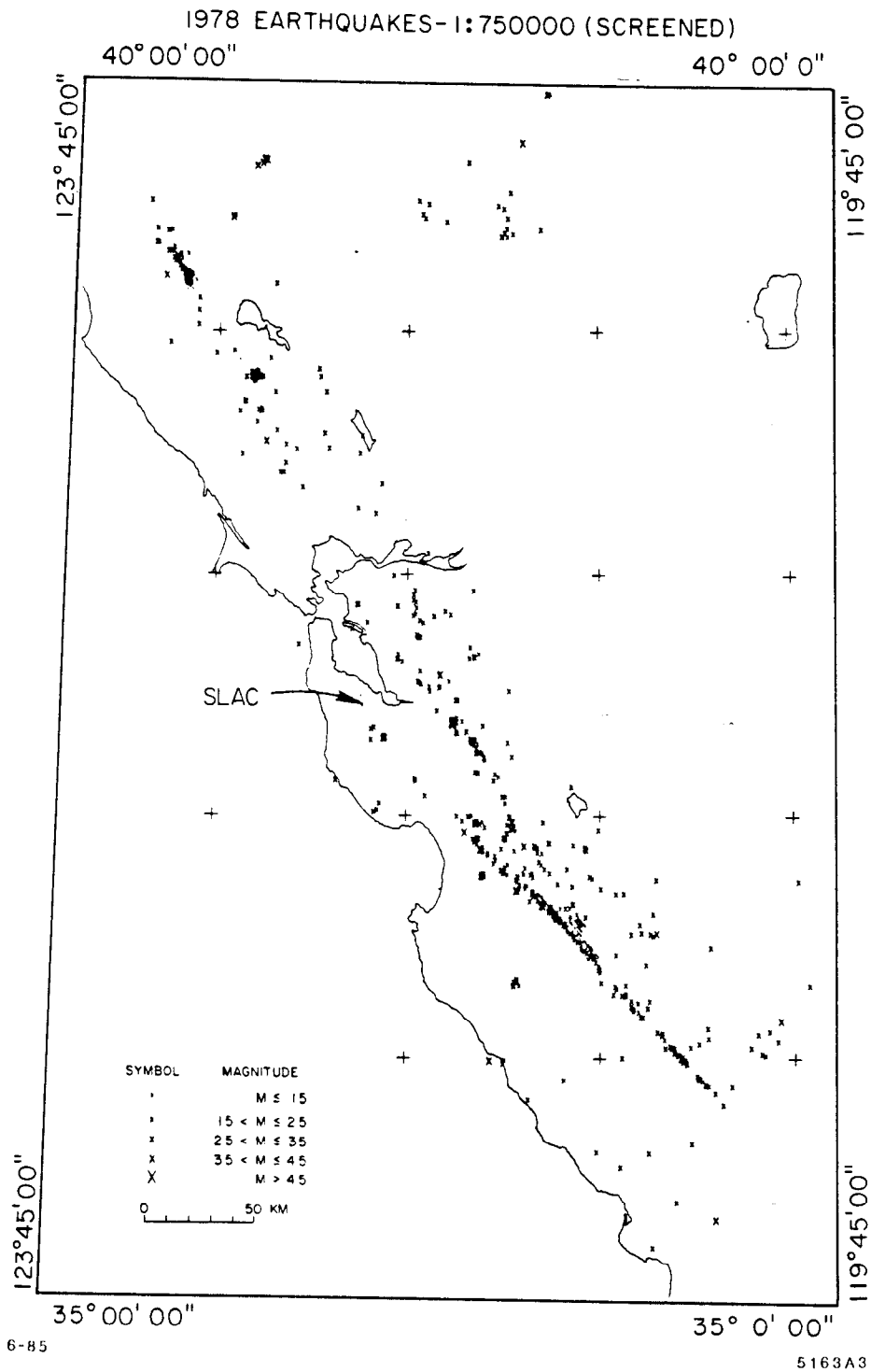
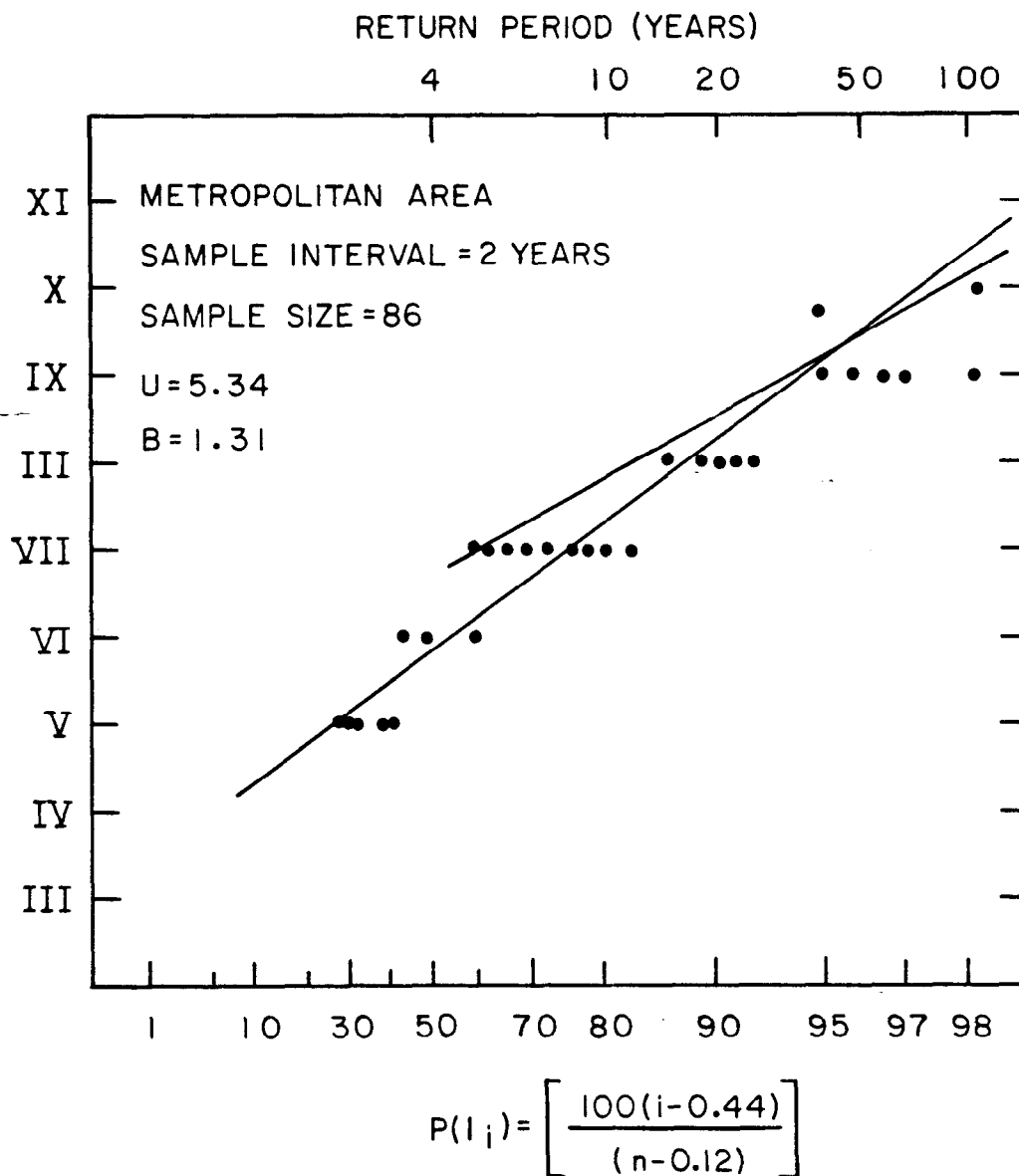


Fig. 2.5. San Andreas Fault Outlined by Earthquakes Detected in 1978 (from Ref. 7).

rock boundary is weak (or lubricated) strain release occurs in many small steps. If a plate boundary is locked, it will take a long time before a catastrophic release takes place. The return period of an event as a function of magnitude for the Bay Area is plotted in Fig. 2.6. The table on the right relates "human perception" of the event to the Richter magnitude scale. Insurance underwriters make use of such data in calculating earthquake premiums in any given geographic location of the country.

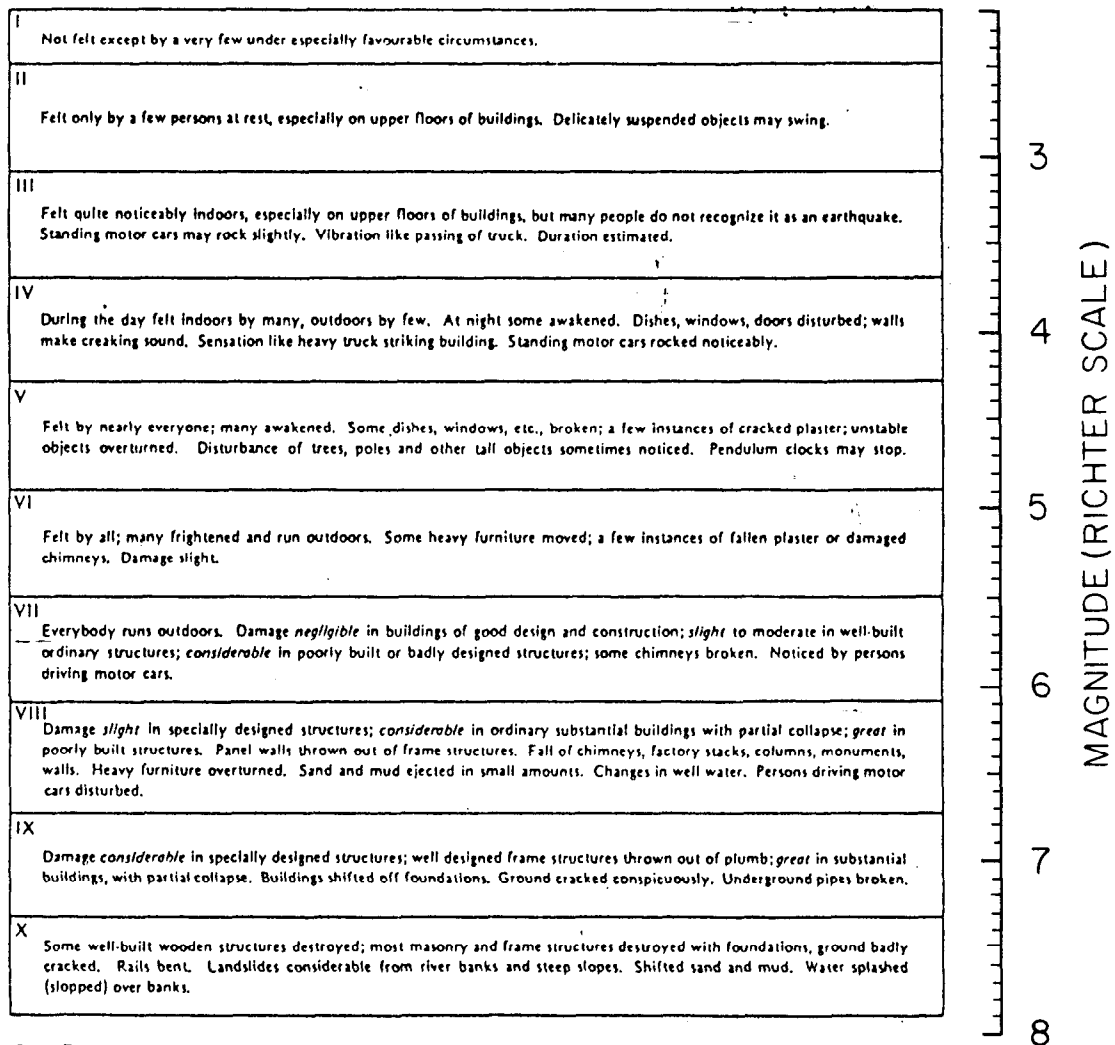


Biannual maximum intensity distribution of earthquakes
San Francisco bay area from 1799 to 1971.

8-85

5163A4

Fig. 2.6(a). Estimated Return Period of Earthquakes of Given Magnitude for the Bay Area (from a report by John A. Blume & Assoc., July 31, 1961).



6-85
5163A5

Fig. 2.6(b). Relationship between Richter Magnitude and the Modified Mercalli Scale (from Ref. 3).

Such data also assists accelerator designers in risk analysis and planning the types of structures and supports that will be necessary to sustain the motion during the project's lifetime. Figure 2.7, for example, depicts an estimate of the maximum ground accelerations that can be expected in earthquakes of given magnitude and distance from epicenter. Aside from setting certain design criteria, the event rates are simply too low to affect the daily operation or performance of a collider.

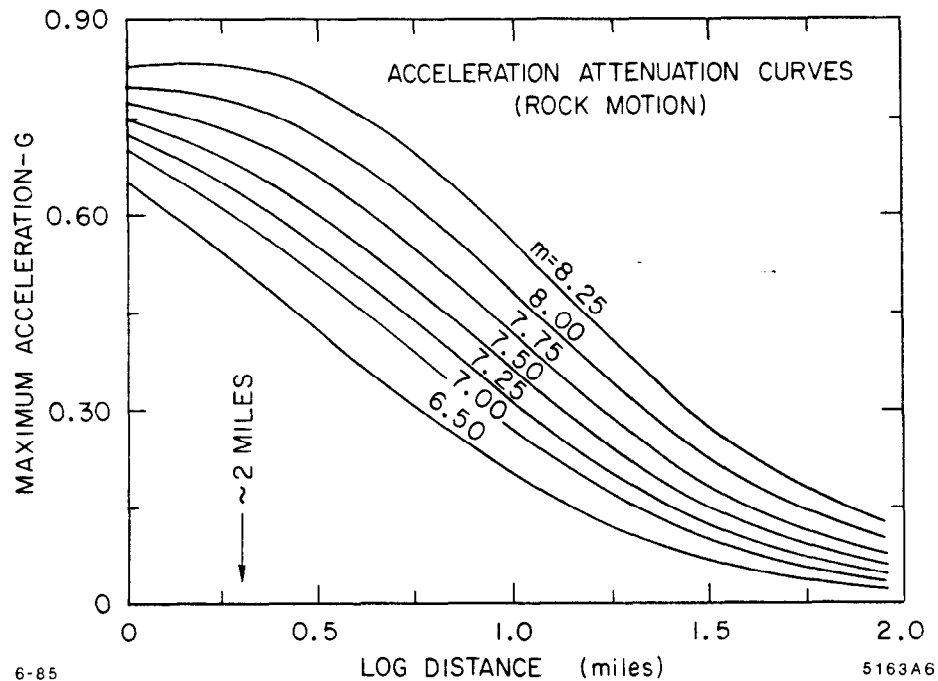


Fig. 2.7. Maximum Ground Acceleration versus Distance from Epicenter (Parameter - Magnitude)(from John A. Blume *ibid*).

2.3.2 Natural Microseismic Noise

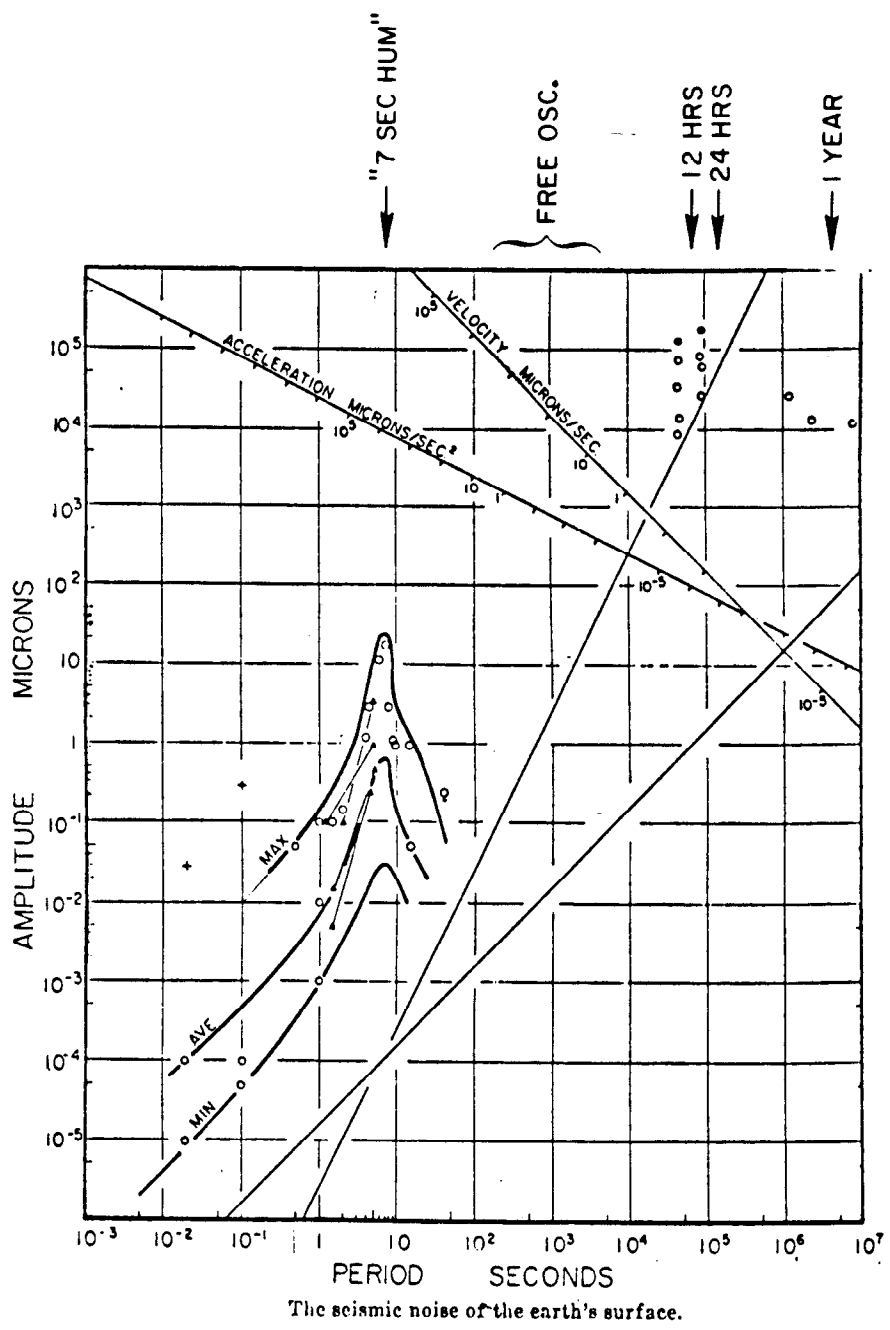
Having spent several pages describing what is *not* the problem, we will devote the rest of the lecture to what *is*, but I must first tell you a funny little story.

Back in the 1950's, when the CERN laboratory in Geneva was thinking about building the Proton Synchrotron (PS), the support engineers decided to build a large concrete "*monolithic*" slab on which to place a long string of magnets. Being careful (CERN engineers are always *very* careful) they decided to measure how much the slab elongated with temperature and distorted as the concrete cured by instrumenting the setup with a collection of position sensors. Much to their amazement, the gauges indicated that the slab "*jiggled*". They had unwittingly built a seismometer. Even more interesting, the amplitude of the noise was correlated with storms arising in the North Sea or in the Bay Biscay, *a half continent away*.

Seismologists had, of course, lived with such noise problems for then past 50 years, but the impetus (and money) to study them occurred in the late 1950's when treaty verification of underground atomic bomb testing became an important issue. Other local natural microseismic noise sources are waterfalls and even wind in the trees and against buildings.

Figure 2.8 (Brune and Oliver, 1959)⁸ displays an early "*qualitative*" and "*averaged*" compilation of the range of noise amplitudes one can expect over a very wide range of frequencies. The dominant feature of concern to us is affectionately called the "*7 second hum*" by seismologists. Another early compilation (Franti et al., 1962)⁸ Fig. 2.9, depicts the higher frequency side of the peak taken from many stations on the American continent. We will examine this disturbance in quantitative detail in Section 4.

Presented as we are with a ground motion spectrum we will engage in what might be called "*forensic seismology*", in order to determine the sources of the disturbances. In this detective story the finger prints - signatures if you wish, are characteristic frequencies and their line widths.



↑ 100Hz

↑ 1 mHz

CHANGES IN ATMOSPHERIC LOADING

6-85

5163A7

Fig. 2.8. Qualitative Display of Ground Noise versus Period (from Ref. 8).

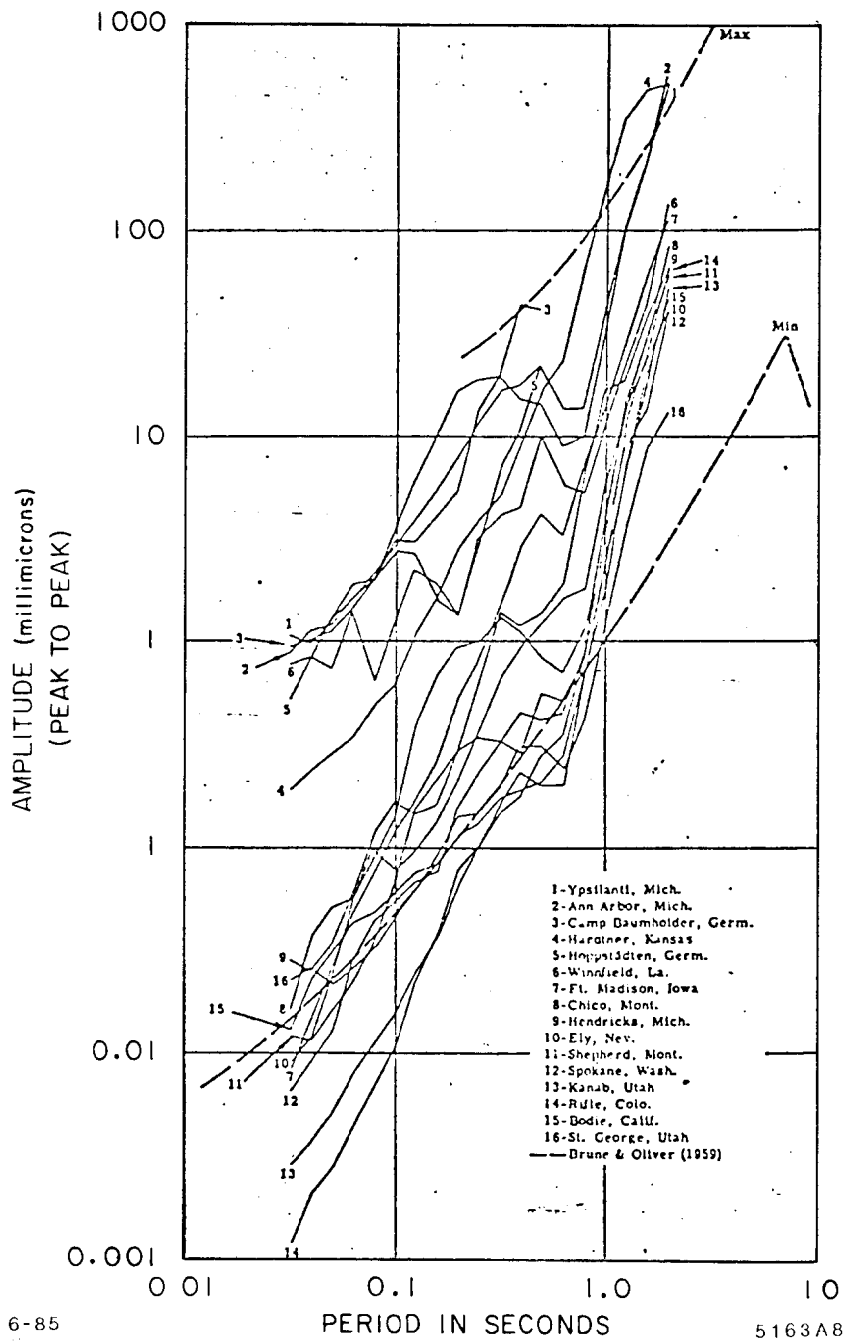


Fig. 2.9. High Frequency Side of the Noise Spectrum (from Ref. 9).

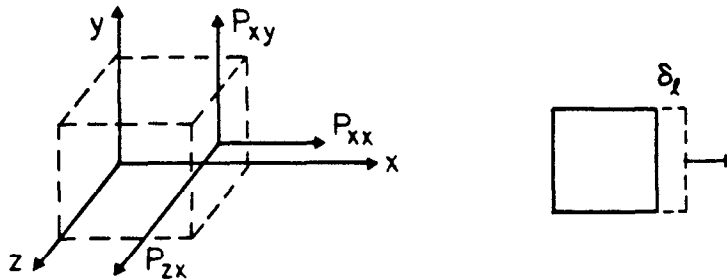
3. A DIGRESSION

In order to appreciate what follows, we must take time out to briefly review two matters – wave propagation and how to work in the frequency domain.

3.1 HOW DOES SOUND PROPAGATE IN AN ELASTIC MEDIUM?

Let us consider a *homogeneous, isotropic* and *elastic* substance and subject it to a generalized stress vector P .

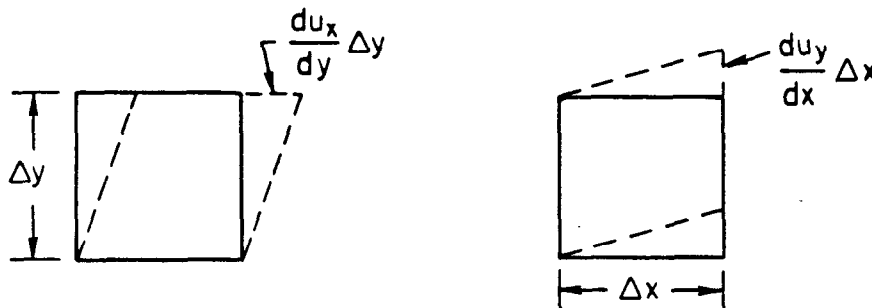
Fig. 3.1. Stress Cube – Illustrating Elongation and Shear Strain.



1. The result of P_{xx} is an elongation δl and we will write that

$$\delta l/l = \epsilon_{xx} = du_x/dx$$

where u is the generalized particle displacement from equilibrium. For an *elastic* medium strain is proportional to stress, i.e., Hook's law is obeyed. If we push in all three directions with P_{xx} , P_{yy} and P_{zz} the volume gets smaller, and the constant of proportionality is the *bulk modulus* k .



2. The two components of simple shear sum to

$$\epsilon_{xy} = \frac{du_x}{dy} + \frac{du_y}{dx}$$

We will use the *shear modulus* μ to linearly relate shear stress and strain.

Using the components in all directions permits the setting up of an equation of motion for the generalized particle displacement from equilibrium:

$$U = i u_x + j u_y + k u_z \quad (1)$$

$$\text{as } \rho \ddot{U} = (k + 4/3\mu) \nabla \nabla \cdot u - \mu (\nabla \times \nabla \times u)$$

in which ρ is the density of the medium.

Special Case 1.

Let us let $\text{curl } u = \nabla \times u = 0$, but $\text{div } u$ finite,

$$\text{since } \nabla \nabla \cdot u = \nabla \cdot \nabla u, \quad \text{then } \frac{d^2 u}{dt^2} = (k + 4/3\mu) / \rho \nabla \cdot \nabla u \quad (2)$$

For a plane wave in the x direction we have:

$$\frac{d^2 u_x}{dt^2} = C^2 \frac{d^2 u_x}{dx^2} \quad (3)$$

a wave equation whose solution is a wave of velocity:

$$C_p = \sqrt{\{(k + 4/3\mu) / \rho\}} \quad (4)$$

This is called the *irrotational* wave, more loosely the *compressional wave*, *longitudinal wave*, *P wave* or *primary wave*.

Special Case 2.

Now let $\text{div } u = \nabla \cdot u = 0$, that means the medium is incompressible. Since $\nabla \times \nabla \times u = \nabla \nabla \cdot u - \nabla \cdot \nabla u = -\nabla \cdot \nabla u$ we can write:

$$\frac{d^2 u}{dt^2} = \frac{\mu}{\rho} \nabla \cdot \nabla u \quad (5)$$

For a plane wave in the x direction we can have particle motions only in the y and z degrees of freedom so:

$$\frac{\partial^2 u_{y,z}}{\partial t^2} = \frac{\mu}{\rho} \frac{\partial^2 u(y,z)}{\partial x^2} \quad (6)$$

The solution to this equation is a *solenoidal* wave or more loosely called the *transverse wave*, *the shear wave*, *the secondary wave* because its velocity:

$$C_s = \sqrt{(\mu/\rho)} \quad \text{is slower.} \quad (7)$$

In general, you get both types, but notice that in a liquid or gas, which have no shear strength, only pressure waves can be supported.

Relationship between the Elastic Constants of a Material

Q: What happens when you pull on a cylinder of steel?

A: Aside from getting longer, it also shrinks in diameter.

The ratio of compressional strain to tensional strain is called Poisson's ratio σ and can be expressed in terms of k and μ by

$$\sigma = \frac{3k - 2\mu}{6k + 2\mu}$$

and therefore must be $\leq 1/2$.

The more familiar Youngs Modulus – the ratio of longitudinal stress/strain is:

$$Y = \frac{9k\mu}{\mu + 3k} = 3k(1 - 2\sigma) = 2\mu(1 + \sigma)$$

Knowing any two of these four quantities for a material permits the calculation of the other two.

-- The velocity ratio $C_p/C_s = \sqrt{(k + 4/3\mu)/\mu}$ is also of interest.

If, for example, $\sigma = 1/4$ as is approximately true for many materials in the earth, then $k = 5/3\mu$ and $C_p/C_s = \sqrt{3} = 1.73$.

Some numerical values for these parameters are shown in Table 3.1.

Table 3.1
Elastic Constants and the Velocity of Sound in Some Materials

Material Quantity	Granite	Shale	Limestone	Miocene Sandstone	Compacted Fill	Santa Clara Formation (Weathered)
$C_p = \sqrt{\frac{k+4/3\mu}{\rho}}$	5-6 km/s	2.2	≈ 6	7000 ft/s	1615 ft/s	2000-3000 ft/s
$C_s = \sqrt{\frac{\mu}{\rho}}$	2-3 km/s	0.81	≈ 3	4500 ft/s	860 ft/s	?
$k = \text{Bulk Modulus}$	3×10^{11} dynes/cm ²					
$\mu = \text{Shear Modulus}$	2×10^{11}			74×10^6	3×10^6	
$\rho = \text{Density}$	2.7 gr/cc			1.91	1.95	
$\sigma = \text{Poisson Ratio}$	0.2-0.3			0.15	0.3	
$C_p/C_s = \text{Velocity Ratio}$	1.63-1.87	2.72	≈ 2.0	1.56	1.88	
$Y = \text{Young's Mod.}$				171×10^6 lbs/ft ²	7.35×10^6 lbs/ft ²	

The earth is neither homogeneous nor isotropic. Waves meeting a discontinuity will reflect and refract. One especially interesting interface is its *surface* (which is not even very flat).

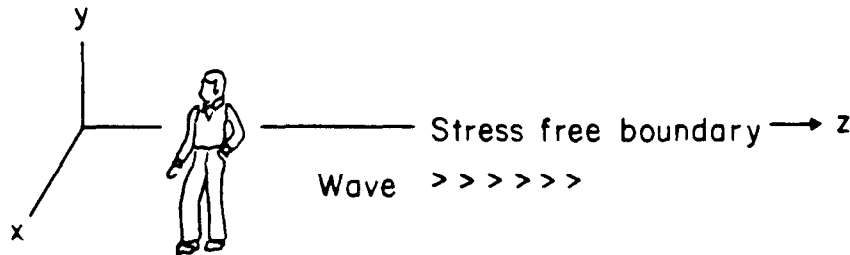


Fig. 3.2. Boundary Conditions for Surface Waves.

Since the potentials of the solution of this boundary value problem decrease exponentially with depth, the disturbances are confined to the neighborhood of the free surface. These surface waves were first calculated in 1886 by John William Strutt, better known to you as Lord Rayleigh. (Fig. 3.3.) The particle motion is an ellipse in the yz plane, that is, we are dealing with a combination of P and vertical shear (SV) waves. For a medium with a velocity ratio $C_p/C_s = 1.7$, the phase velocity of a Rayleigh wave is about $0.92C_s$.

If the medium consists of a surface layer on top of one of higher wave velocity, a common situation, surface waves polarized in the zx plane can be supported. These are called Love waves and are sometimes designated LQ . L for Love, Q for quer, the German word for transverse. ($C_{LQ} \approx 4.43$ km/sec, $C_R \approx 3.97$ km/sec, somewhat faster across the Pacific Ocean Floor).

Needless to say, from here on the situation gets more complicated almost an art form, when considering layered, non-isotropic, even nonlinear media on a local scale. The saving grace when timing earthquakes with very long waves is that the earth's heterogeneity is averaged out. We will discuss attenuation later on.



8-85

5163A35

Fig. 3.3. John William Strutt (Lord Rayleigh).

3.2 PROPERTIES OF THE FOURIER TRANSFORM

We have already noted that we will find it convenient to characterize the identity of a ground motion by its spectrum. Just as important, if not more so, is how the motion affects the beam in an accelerator. In the analysis of electrical circuitry and mechanical structures, it is often convenient to work in the frequency domain. In other words, the

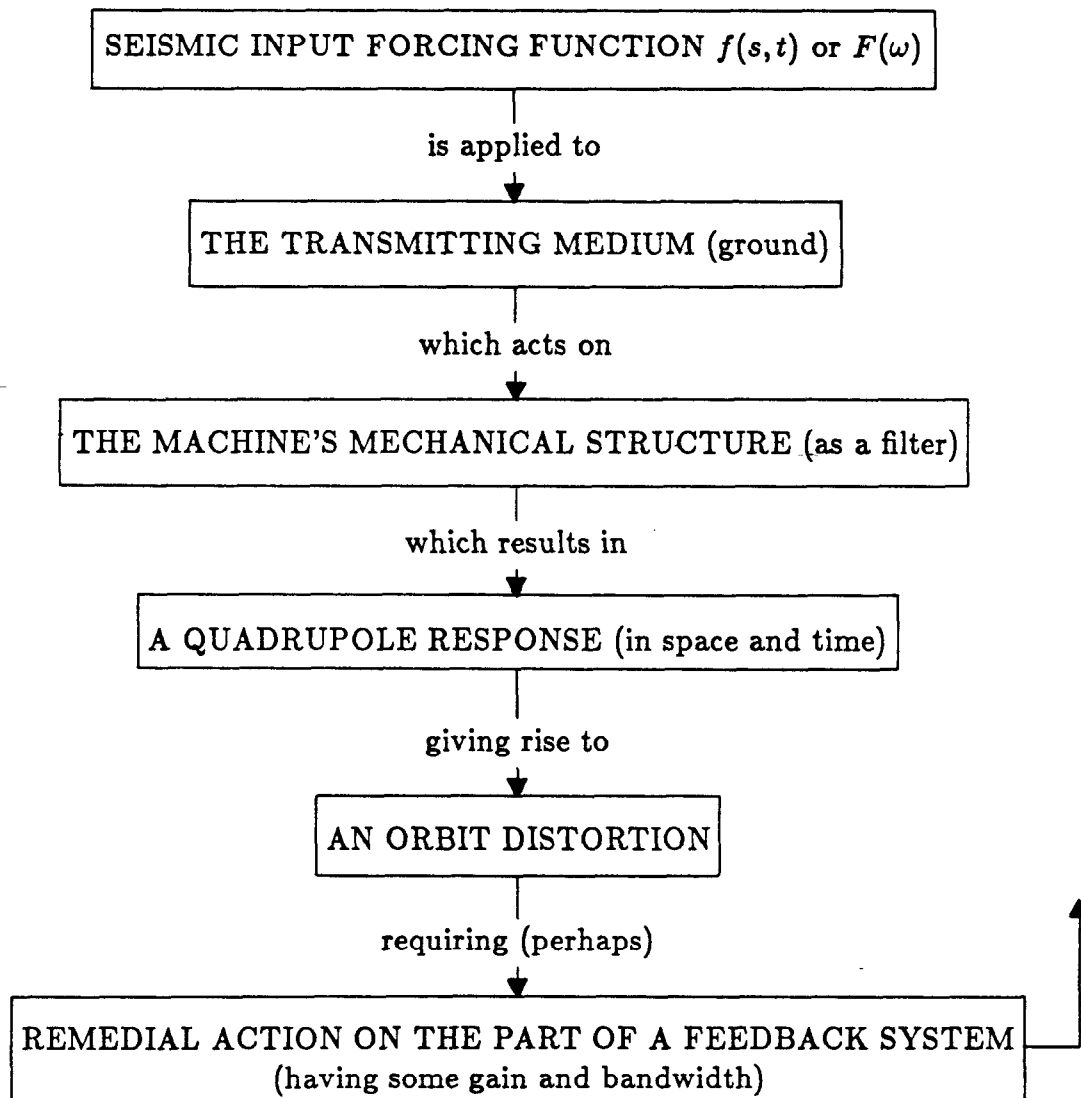


Fig. 3.4. Application of the Fourier Forcing Function.

The *Fourier Transform* $H(f)$ of the function $h(t)$ is defined here as:¹⁰

$$H(f) = \int_{-\infty}^{+\infty} h(t) e^{i2\pi ft} dt$$

and is a *complex quantity*

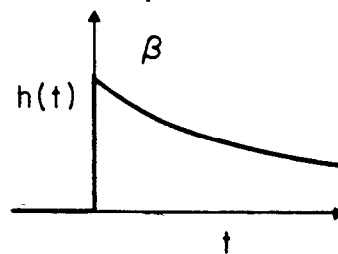
$$H(f) = R(f) + iI(f) = |H(f)| e^{i\Theta(f)}$$

$$|H(f)| = \sqrt{R^2 + I^2}$$

$$\Theta(f) = \tan^{-1} \frac{I(f)}{R(f)}$$

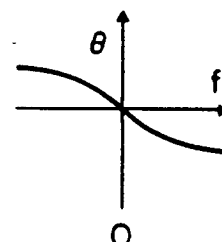
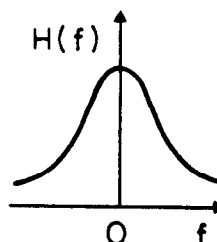
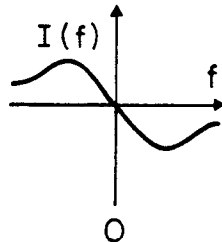
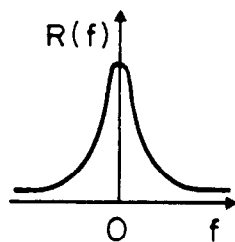
If, for example,

$$h(t) = \begin{cases} \beta e^{-\alpha t} & t > 0 \\ 0 & t < 0 \end{cases}$$



then

$$\begin{aligned} H(f) &= \int_0^{\infty} \beta e^{-\alpha t} e^{-i2\pi ft} dt = \beta \int_0^{\infty} e^{-(\alpha + i2\pi f)t} dt \\ &= -\frac{\beta}{\alpha + i2\pi f} e^{-(\alpha + i2\pi f)t} \Big|_0^{\infty} = +\frac{\beta}{\alpha + i2\pi f} \\ &= \frac{\beta\alpha}{\alpha^2 + (2\pi f)^2} - j \frac{2\pi f\beta}{\alpha^2 + (2\pi f)^2} = \frac{\beta}{\sqrt{\alpha^2 + (2\pi f)^2}} e^{i \tan^{-1}(2\pi f/\alpha)} \end{aligned}$$



Conversely, or inversely if you like, the Inverse Fourier Transform is:

$$h(t) = \int_{-\infty}^{+\infty} H(f) e^{i2\pi ft} df$$

Exercise: Given $H(f) = \exp - |2\pi f|$, find $h(t)$.

A useful compilation of Fourier Transform pairs is shown in Tables 3.2 and 3.3. Note in particular the transforms of delta functions both in time and frequency and that gaussian distributions transform into gaussians. Doesn't this remind you of Heisenberg? Other useful (like additivity and symmetry) properties are summarized in Table 3.4, but we need two more integrals.

The Convolution Integral of $x(t)$ and $h(t)$ is:

$$y(t) = \int_{-\infty}^{+\infty} x(\tau) \cdot h(t - \tau) d\tau = x(t) * h(t)$$

with this *overlap* integral we can prove that:

$$h(t) * x(t) \longleftrightarrow H(f) X(f)$$

$$h(t) \cdot x(t) \longleftrightarrow H(f) * X(f)$$

This is called the *Convolution Theorem*. With the Convolution Theorem one can also prove that

$$\int_{-\infty}^{+\infty} h^2(t) \cdot dt = \int_{-\infty}^{+\infty} |H(f)|^2 df$$

which is called *Parseval's* theorem which states that the total energy computed in the time domain must *equal* the total energy in the frequency domain. Notice that we are now dealing with real *power* (a scalar) i.e., whatever phase information there was, is no longer present.

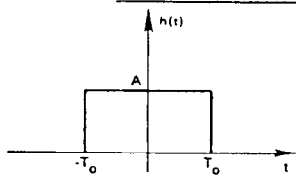
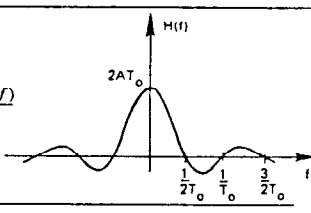
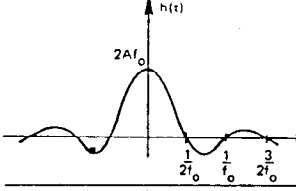
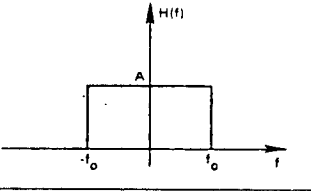
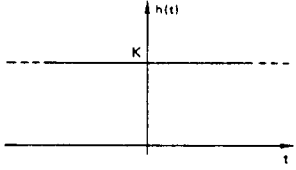
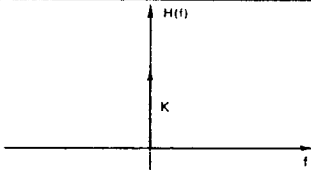
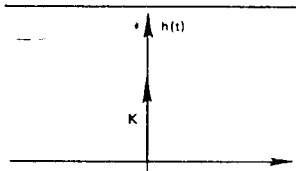
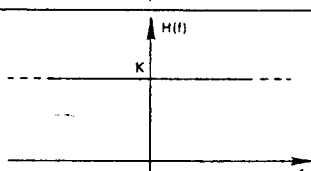
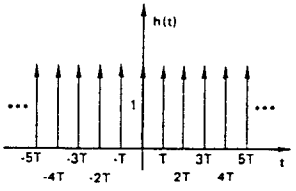
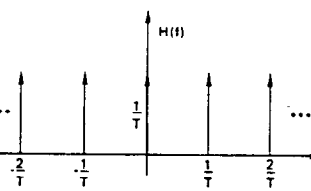
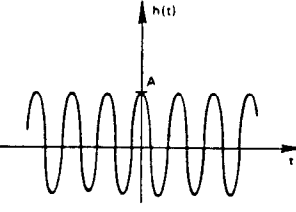
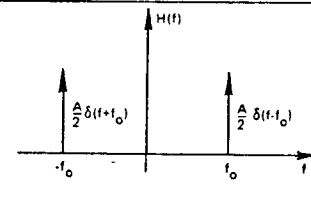
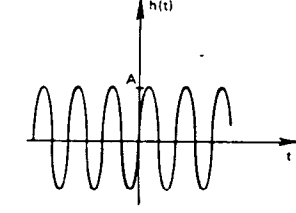
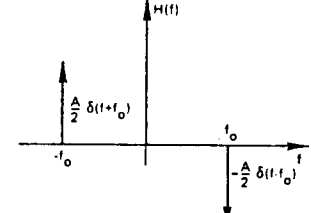
Exercise: With respect to ground motion studies, in what physical units would you plot a power spectrum?

The Correlation Integral of $x(t)$ and $h(t)$ is defined as:

$$z(t) = \int_{-\infty}^{+\infty} x(t) h(t + \tau) d\tau$$

if $x(t) \neq h(t)$, then this integral is called the crosscorr. of $x(t)$, $h(t)$
if $x(t) = h(t)$, then this integral is called the autocorrelation of x , h .

Table 3.2. Table of Fourier Transform Pairs (from Ref. 10)

Time domain		Frequency domain
	$h(t) = \begin{cases} A & t < T_0 \\ \frac{A}{2} & t = T_0 \\ 0 & t > T_0 \end{cases}$	 $H(f) = 2AT_0 \frac{\sin(2\pi T_0 f)}{2\pi T_0 f}$
	$h(t) = 2Af_0 \frac{\sin(2\pi f_0 t)}{2\pi f_0 t}$	 $H(f) = \begin{cases} A & f < f_0 \\ \frac{A}{2} & f = f_0 \\ 0 & f > f_0 \end{cases}$
	$h(t) = K$	 $H(f) = K\delta(f)$
	$h(t) = K\delta(t)$	 $H(f) = K$
	$h(t) = \sum_{n=-\infty}^{\infty} \delta(t - nT)$	 $H(f) = \frac{1}{T} \sum_{n=-\infty}^{\infty} \delta\left(f - \frac{n}{T}\right)$
	$h(t) = A \cos(2\pi f_0 t)$	 $H(f) = \frac{A}{2} \delta(f - f_0) + \frac{A}{2} \delta(f + f_0)$
	$h(t) = A \sin(2\pi f_0 t)$	 $H(f) = -j\frac{A}{2} \delta(f - f_0) + j\frac{A}{2} \delta(f + f_0)$

6-85

5163A11

6-85

5163A12

Table 3.3. Table of Fourier Transform Pairs (continued)

Time domain		Frequency domain
	$h(t) = -\frac{A^2}{2T_0}t + A^2$ $= 0 \quad t > 2T_0$	$H(f) = A^2 \frac{\sin^2(2\pi T_0 f)}{(\pi f)^2}$
	$h(t) = A \cos(2\pi f_0 t)$ $= 0 \quad t > T_0$	$H(f) = A^2 T_0 [Q(f + f_0) + Q(f - f_0)]$ $Q(f) = \frac{\sin(2\pi T_0 f)}{2\pi T_0 f}$
	$h(t) = \frac{1}{2}q(t) + \frac{1}{4}q\left(t + \frac{1}{2f_c}\right) + \frac{1}{4}q\left(t - \frac{1}{2f_c}\right)$ $q(t) = \frac{\sin(2\pi f_c t)}{\pi t}$	$H(f) = \frac{1}{2} + \frac{1}{2} \cos\left(\frac{\pi f}{f_c}\right)$ $= 0 \quad f > f_c$
	$h(t) = \frac{1}{2} + \frac{1}{2} \cos\left(\frac{\pi t}{T_0}\right)$ $= 0 \quad t > T_0$	$H(f) = \frac{1}{2} Q(f) + \frac{1}{4} [Q\left(f + \frac{1}{2T_0}\right) + Q\left(f - \frac{1}{2T_0}\right)]$ $Q(f) = \frac{\sin(2\pi T_0 f)}{\pi f}$
	$h(t) = \frac{1}{2} \alpha \exp(-\alpha t)$	$H(f) = \frac{\alpha^2}{\alpha^2 + 4\pi^2 f^2}$
	$h(t) = \left(\frac{\alpha}{\pi}\right)^{1/2} \exp(-\alpha t^2)$	$H(f) = \exp\left(-\frac{\pi^2 f^2}{\alpha}\right)$

6-85

5163A10

6-85

5163A9

Table 3.4. Useful Properties of the Fourier Transform (from Ref. 10)

SUMMARY OF PROPERTIES

For future reference the basic properties of the Fourier transform are summarized in Table 3-2. These relationships will be of considerable importance throughout the remainder of this book.

PROPERTIES OF FOURIER TRANSFORMS		
Time domain	Equation no.	Frequency domain
Linear addition $x(t) + y(t)$	(3-2)	Linear addition $X(f) + Y(f)$
Symmetry $H(t)$	(3-6)	Symmetry $h(-f)$
Time scaling $h(kt)$	(3-12)	Inverse scale change $\frac{1}{k} H\left(\frac{f}{k}\right)$
Inverse scale change $\frac{1}{k} h\left(\frac{t}{k}\right)$	(3-14)	Frequency scaling $H(kf)$
Time shifting $h(t - t_0)$	(3-21)	Phase shift $H(f)e^{-j2\pi ft_0}$
Modulation $h(t)e^{j2\pi ft_0}$	(3-23)	Frequency shifting $H(f - f_0)$
Even function $h_e(t)$	(3-27)	Real function $H_e(f) = R_e(f)$
Odd function $h_o(t)$	(3-30)	Imaginary $H_o(f) = jI_o(f)$
Real function $h(t) = h_r(t)$	(3-43) (3-44)	Real part even Imaginary part odd $H(f) = R_e(f) + jI_o(f)$
Imaginary function $h(t) = jh_i(t)$	(3-45) (3-46)	Real part odd Imaginary part even $H(f) = R_o(f) + jI_e(f)$

Exercise: Calculate the autocorrelation of a *white noise* disturbance.

The Sampling Theorem

We are now in a position to apply these notions to our problem. We will do so graphically. Consider Fig. 3.5. Let us say that $h(t)$ represents a ground motion induced orbit distortion, and that a beam position instrument looks at the motion when the beam goes by at an interval rate depicted by $\Delta(t)$.

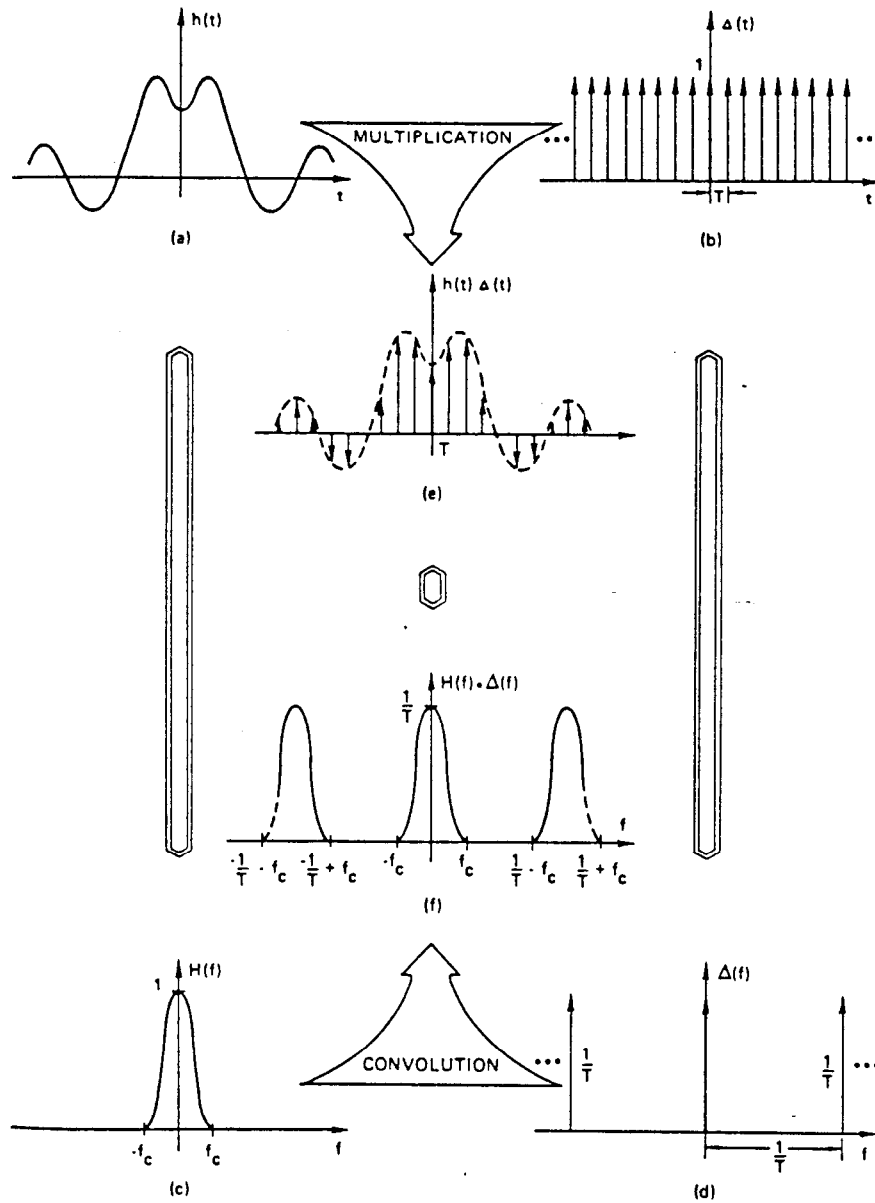
A fairly accurate representation, $h(t) \cdot \Delta(t)$ results in the time domain. In the frequency domain $H(f)$ is convoluted with $\Delta(f)$ to produce $H(f) * \Delta(f)$, which is of course the Fourier Transform of $h(t) \cdot \Delta(t)$. We note that the informational content of Fig. (c) is identical to Fig. (f), i.e., the representation is accurate.

Now consider Fig. 3.6. If we reduce the number of times one can observe the beam, i.e., reduce the *bandwidth* of the observer, Fig. (c) is not accurately represented by Fig. (f), nor for that matter does (e) represent (a), we have lost the higher frequencies. The feedback system that is supposed to "*correct*" the error will begin to zig when it should zag.

The limiting case in which we have just barely enough information is shown in Fig. 3.7 and demonstrates the "*sampling theorem*" graphically. It says that no components of a wave form greater than $f/2$ can be accurately reconstructed if the sampling frequency is f . When the gain of the feedback system is considered the bandwidth of the correcting system is restricted by another factor of $\approx \pi$.

Let me repeat myself... in accelerators this implies that we must have beam sampling repetition rates or circulating frequencies about 6 times higher than the frequencies of the disturbances that we are trying to measure and combat.

FOURIER SERIES AND SAMPLED WAVEFORMS

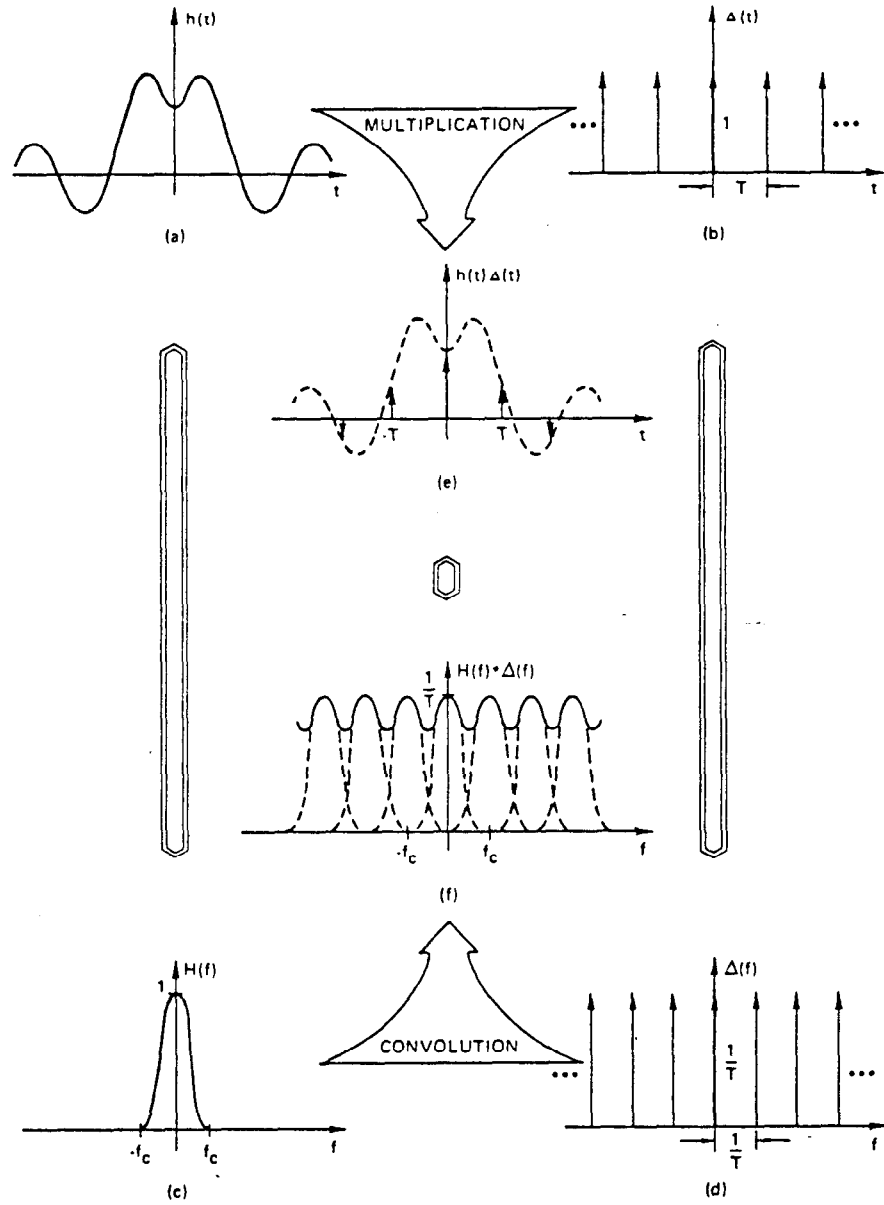


6-85

Graphical frequency convolution theorem development of the Fourier transform of a sampled waveform. 5 163 A 13

Fig. 3.5. A Well Sampled Waveform (from Ref. 10).

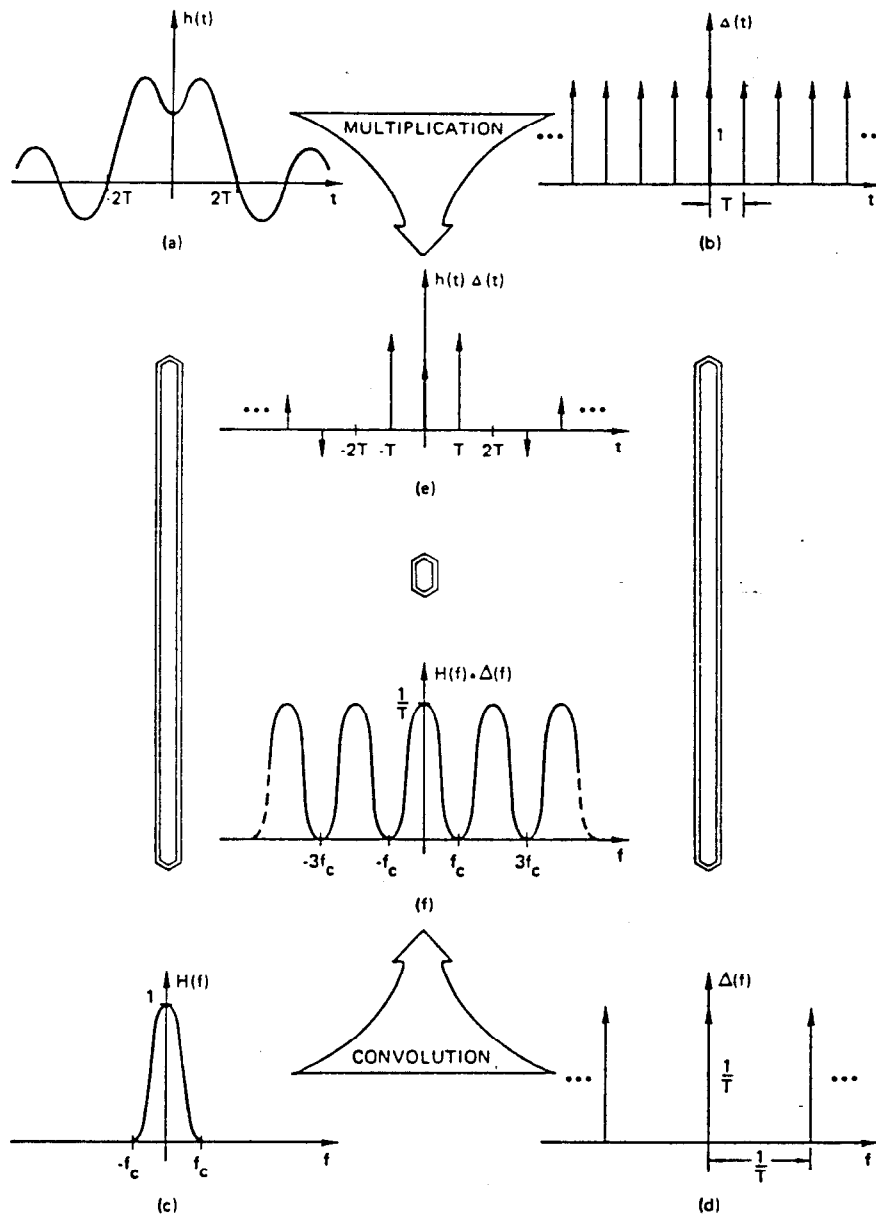
FOURIER SERIES AND SAMPLED WAVEFORMS



6-85 Aliased Fourier transform of a waveform sampled at an insufficient rate. 5163A14

Fig. 3.6. A Badly Sampled Waveform.

FOURIER SERIES AND SAMPLED WAVEFORMS



6-85

Fourier transform of a waveform sampled at the Nyquist sampling rate.

5163A 15

Fig. 3.7. A Waveform Sampled at the Critical Frequency.

4. FREQUENCIES OF INTEREST

We have already noted that if the source frequency is very low (as in earth tides) the whole site moves monolithically and no relative quad displacements result. The situation is more interesting when the wavelength of the ground motion becomes comparable to the dimensions of the accelerator as a whole or perhaps more locally, to the betatron wavelength. To calculate this we need to know the effective velocity of the motion.

In a homogeneous medium the body wave phase velocities are nondispersive and simply calculable from the medium's known elastic constants. Surface (Rayleigh, Love) waves, however, sample the medium to a depth comparable to a wavelength, a depth over which the medium's parameters may vary greatly. (This is discussed in Section 6 below). The effective velocities must therefore be estimated iteratively, taking into account the locations of the source and receiver. To give us a feeling for dimensions, Table 4.1 lists frequencies of interest assuming a relatively low velocity of 2500 ft/sec. The 7 second hum (.15 Hz) will affect the larger machines. Except in the case of the Linear Collider running in test mode, the beam sampling rate is sufficient to measure the effects correctly.

In an excellent modern textbook on "*Quantitative Seismology*" (Aki and Richards, 1980)¹¹ you will find a plot reproduced here as Fig. 4.1, depicting the *Power Spectral Density* of ground noise in one of our regions of interest. The observer's stations are sited on hard rock. The data represents a long term averaged spectrum. The units are velocity²/Hz. Taking the central frequency of the large peak as .15 Hz and integrating the density over a band of full width at half maximum of .15 Hz, one obtains a velocity of about 10^{-4} cm/sec or a time averaged rms displacement at .15 Hz of about 1 micron. Notice the high frequency side of the *power* spectrum falls as $1/f^2$.

What kind of a source produces such a spectrum? On page 85 of his text on the application of Fourier Transforms (Champaney 1973)¹² discusses the function $f(t) = \exp i\{w_0 t + \phi(t)\}$ in which $\phi(t)$ is a stationary *random* function of time. In other words, there is a harmonic driver of frequency w_0 whose phase suffers sudden changes at *random* time intervals. If on the average, there are ν phase changes per time the *power* density spectrum has the form:

$$P_f(w) = \frac{2\nu}{\nu^2 + (w - w_0)^2}$$

in units of power/unit frequency interval.

In this case the width is given by the average frequency of occurrence of the phase jumps. Do *not*, as I did at first, confuse this with the case of the damped harmonic oscillator whose *amplitude* not *power* spectrum has this form.

Table 4.1. Diameters of Various Machine and Frequencies of Interest

Machine	Diameter		Revolution Frequency	Repetition Rate	Frequency at which $\lambda = 0$ $\nu = 2500 \text{ ft/sec}$	
	meters	feet				
SPEAR	74.6	245	1.28 MHz	—	10 Hz	
PEP	700	2296	136 kHz	—	1 Hz	
SLC ARCS	853	2000	—	180 pps test mode 1 pps	1 Hz	
TEVATRON	2 km	6560	47 kHz	—	0.3 Hz	
20 TeV SSC	2.5T	62 km	200000	1.5 kHz	—	0.01 Hz
	10T	16 km	53000	6.0 kHz	—	0.05 Hz
1 × 1 SSLC	2 × 8 km	53000	—	140 pps test mode 1 pps	0.05 Hz	

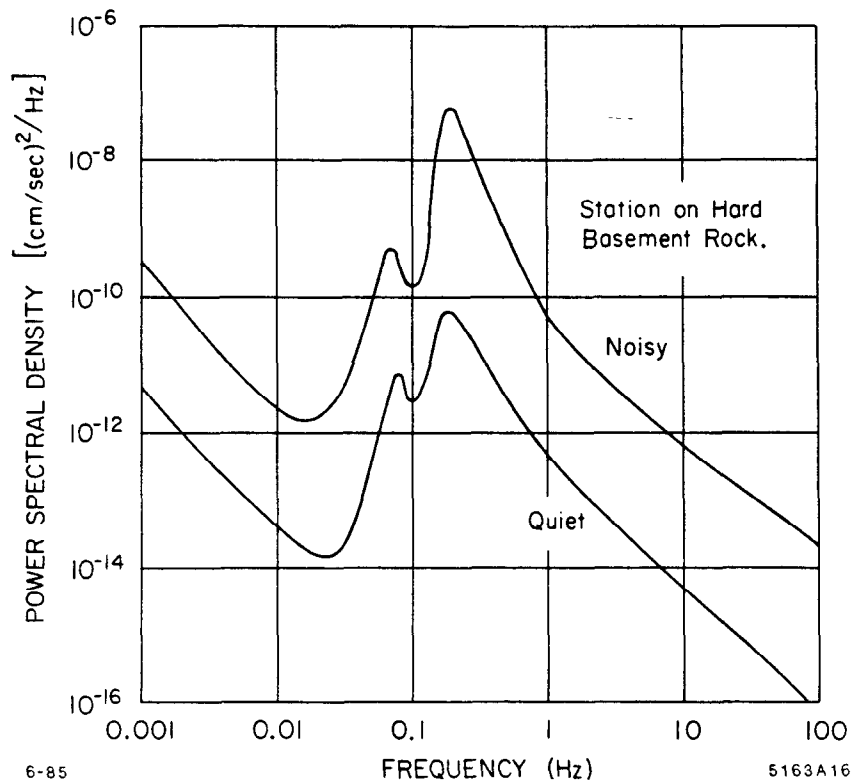


Fig. 4.1. Long Term Averaged "Maximum" and "Minimum" Noise Power Spectra (from Ref. 11).

Just for fun, I have taken the *noisy* time averaged power spectrum for a bed-rock station shown in Fig. 4.1 and fit it with the above form. The resulting fit and its parameters are shown in Fig. 4.2. On this log-log plot the width of the peak appears quite broad, but this is deceiving. On a linear-linear plot (Fig. 4.3) the rather sharp nature of the disturbance is more evident. All this fitting should not be taken too seriously because just as there is no *standard earthquake*, there is no standard microseismic noise spectrum.

One more comment – In dealing with stationary *random* functions we can only talk about Power Spectra, root mean square values and autocorrelation functions. We cannot talk about the Fourier Transform of a stationary random function – *it does not exist* (Ref. 12, page 79). Now, who or what is the driver?

If you live in California and turn on the radio in the morning to the marine weather forecast you might hear the following: – 'local patches of fog, the winds are westerly at 15 knots, sea swell at Point Sur is 4 feet with a period of 10 seconds'. If you look in the sailors' bible, the "American Practical Navigator," you find (on page 791 of the 1977 edition)¹³ that such a wave expends 35,000 horse power per mile of beach.

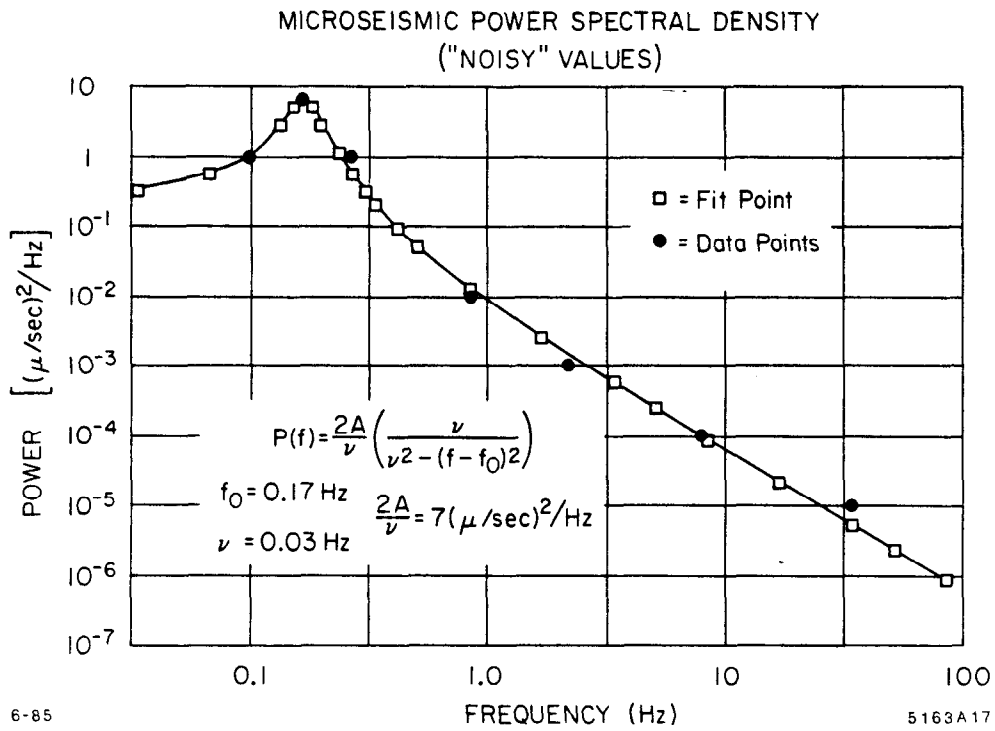


Fig. 4.2. Fit to Maximum Power Spectrum of Fig. 4.1 (Log-Log Scale).

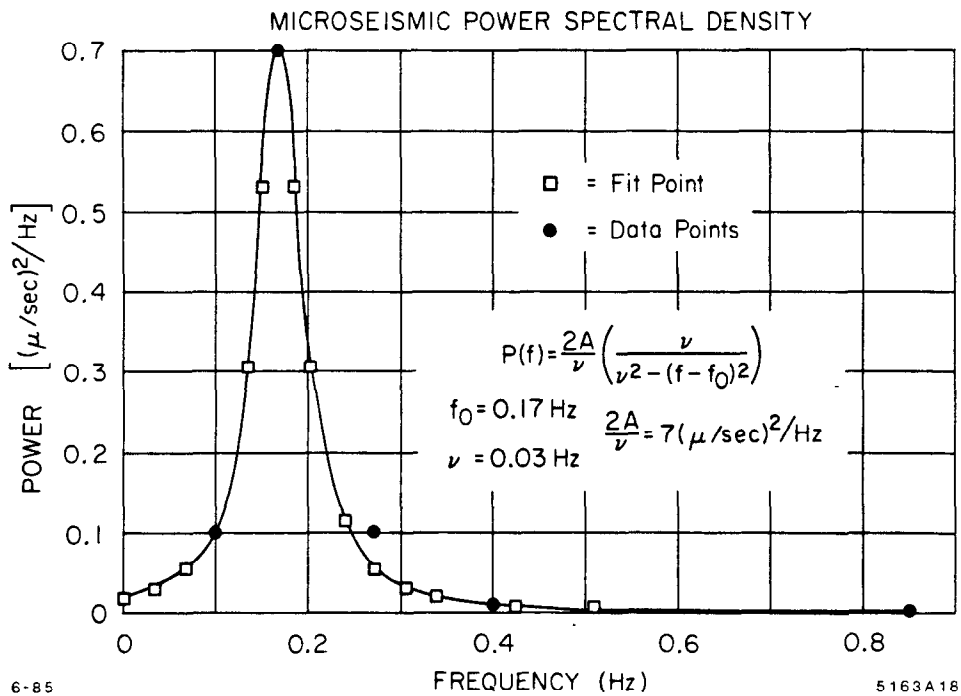


Fig. 4.3. Fit to Maximum Power Spectrum of Fig. 4.1 (Linear Scales).

The ocean wave theory of microseism generation was advanced as long ago as 1904, but, in my mind, a definitive local experiment was performed by Haubrich, Munk and Snodgrass of La Jolla in 1963,¹⁴ who found following a storm a beautiful correlation between local ocean swell on shallow shores and the lower frequency seismic peak, called PF (P for primary). The higher frequency peak DF, containing perhaps 100 times as much energy, has double the frequency and stems from the generation of oppositely directed waves off shore. The frequencies of bands PF, DF change with the age (in days) of a storm which may be thousands of miles at sea.

On a short time scale these two peaks may be remarkably narrow ($Q = f/2\Delta f \approx 14$) indicating that the *beam* of waves was narrow and the length of the coastal strip was of order 100 miles. Waves traveling normal to the coast reach into the continent. A complete and quantitative theoretical analysis of how ocean waves couple to the ground was then published by Hasselmann in 1963,¹⁵ and compared with the data. He concludes that "appreciable microseisms are generated only by Fourier components of random exciting fields that have the same phase velocities as free modes of the elastic system."

--In 1969, Haubrich and McCamy¹⁶ report on studies with a well instrumented Large Aperture Seismic Array (LASA) (you can imagine what it is used for) located in eastern Montana. With this device, which has stations 100 km apart, they can unscramble Rayleigh, Love surface waves as well as high speed compressional body waves and measure their directions and velocities. A lot of what they see travels eastward at a velocity of around 3 km/sec and 4 km/sec, but it is important to read their paper in detail since it provides us with the solution to our problem, namely, a correlated measurement of the waves in direction and time. Since the instantaneous coherence of the wave trains appears to be high, even for inland locations, with an array of sensors one should be able to perform *real time* reconstruction of the disturbances. You may imagine a certain high level of computational power would be required, but given modern computers this should not be too difficult today. Attenuation between coasts and into the continent is only about 10 db.

Aside from storms, from which no region is immune, are there places in the country that are exceptionally quiet? The people who test modern inertial guidance systems need such places.¹⁷ I am told that there are a few -- one in Texas. When asked, *why there?* the answer was, *there is nobody out there!* Which brings us to the next subject.

5. SOME MEASUREMENTS AT SLAC

The question that we will address in this section is *what does one measure in and around a populated laboratory?* Unfortunately – a lot!

5.1 INSTRUMENTATION

5.1.1 Sensors

Figure 5.1(a) depicts *bore hole* geophones, (vertical and horizontal) which are easily carried about. Inside the case, a 1 kg mass is suspended on a spring having an undamped natural period of 1.0 Hz. Acting like an inverse loud speaker, the generated signal voltage is proportional to velocity. Externally damped by a shunt resistor, its velocity response is nearly flat from 2 to 50 Hz. With a sensitivity of 1 volt/cm/sec it is easy to measure amplitudes down to 10^{-3} microns. Figure 5.1(b) depicts a horizontal long period seismometer in the form of a horizontal pendulum whose period is adjusted, from say 5 to 30 seconds, by means of its levelling screws. Electrically it behaves in the same manner as the short period device.

5.1.2 Data Display and Recording

Aside from the usual instruments such as oscilloscopes and chart recorders, the essential device is a *Fast Fourier Transform Analyzer* (FFTA) with two input channels. Several commercial devices are capable, among many other things, of measuring the complex fourier *Transfer-Functions* of *transient* and time averaged signals and graphically displaying the results in magnitude and phase. Other function displays of their substantial on-board computers are listed in Table 5.1.¹⁸ There are many devices of this kind which are widely used in such varied and important applications as predicting when heavy rotating machinery bearings wear out, structural analysis, vibration isolation, instability diagnostics of accelerator beams and even listening to whales and/or submarines.

5.2 DATA

5.2.1 Base Levels

When you place a seismometer on the ground or on a tunnel floor and look at a velocity signal that has been amplified and integrated once so it is proportional to amplitude, on a chart recorder you see what is shown in Fig. 5.2(a). Footsteps or a person jumping are clearly seen. At 6pm after everyone has gone home, it looks like Fig. 5.2(b). Clearly when you get right down to earth you see a lot of *dirt* effects! If now you put the signal into a *true reading* rms voltmeter to measure sqrt noise power and filter out the *high frequency* disturbances you see

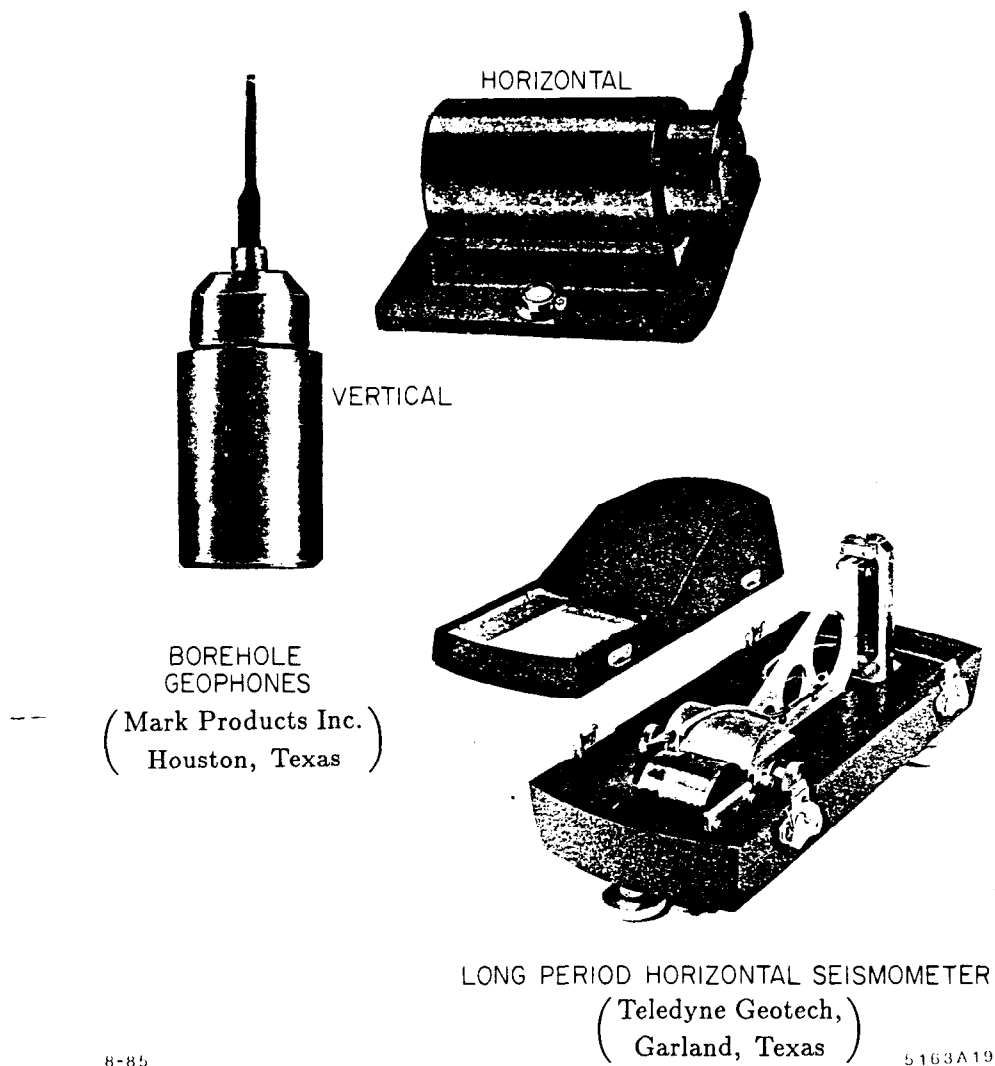


Fig. 5.1. Instruments for Ground Noise Investigation.

over a weekend what is displayed in Fig. 5.3(a). In the underground tunnel it's pretty quiet, but every now and then there are substantial signals. If you take the apparatus to the surface near an off-site road, you see Fig. 5.3(b). Notice the dips between midnight and 6 a.m. (especially between Sunday night and Monday morning). Everyone must be in bed! Let us call this the base level.

Figure 5.3.1 depicts a typical horizontal root mean square *amplitude* spectral density taken in the PEP tunnel about 75 feet under ground. The peak at 6 Hz is due to a steadily running compressor located 1/2 mile away.

Table 5.1(a). Fast Fourier Transform Analyzer Display Functions (from Ref. 18)

DEFINITIONS OF FUNCTIONS		
DISPLAY SELECT	FUNCTION COMPUTED	DESCRIPTION
Coherent Output Power (COP) LOG	$COP = \frac{G_{AB} \cdot G_{AB}^*}{G_{AA}}$ $= \gamma^2_{AB} G_{BB}$ $10 \text{ LOG}_{10} COP$	Coherent output power (COP) spectrum indicates power in signal, B(t), that is coherent with signal, A(t). Total power spectrum G _{BB} , indicates entire content of B(t) while COP indicates only that portion caused by A(t) thru a linear process. When B(t) is caused by unrelated multiple inputs, COP indicates only that portion due to single input, A(t).
Coherence (COH)	$\gamma^2_{AB} = \frac{G_{AB} \cdot G_{AB}^*}{G_{AA} \cdot G_{BB}}$ $= \frac{ G_{AB} ^2}{G_{AA} \cdot G_{BB}}$	Real Spectrum "power squared" ratio indicates linear cause/effect relationship between A(t) and B(t). Linear transmission system excited only by A(t) yields $\gamma_{AB}^2 = 1$ at all frequencies. Non-linearities or inputs in addition to A(t) produce γ_{AB}^2 between "0" and "1".
Auto-Correlation Function (Δ) (Auto Corr. - ACF)	$R_{AA}(\tau) = \mathcal{F}^{-1}\{G_{AA}\}$ $= \frac{1}{P} \int_0^P A(t) \cdot A(t+\tau) dt$	Time domain statistic comparing similarity of A(t) to replicates of itself, delayed by time, τ. At τ = 0, R _{AA} = mean square of A(t). As τ → ∞, R _{AA} approaches square of mean value. Oscillations in R _{AA} indicate bandwidth and periodicity of A(t).
Cross-Correlation Function (X Corr. - CCF)	$R_{AB}(\tau) = \mathcal{F}^{-1}\{G_{AB}\}$ $= \frac{1}{P} \int_0^P A(t)B(t+\tau) dt$	Time statistic comparing similarity of A(t) and B(t). Value of τ that maximizes R _{AB} indicates time lag between signals. Maximum value of R _{AB} divided by square root of [R _{AA} (0)] [R _{BB} (0)] yields correlation coefficient (equal to 1 for identical signals, 0 for unrelated signals).
Signal Enhancement (Δ) (Avg. Time - AT)	$\bar{A}(t)$	Ensemble averaged time histories computed at each time point across a series of instantaneous time histories, each triggered from a common condition. Used to extract mean value time history.
Linear Spectrum (Δ) (Inst. Spec. - IS) LIN MAG LOG MAG PHASE REAL IMAG	$S_{\bar{A}} = \mathcal{F}\{A(t)\}$ $= S_{\bar{A}} \cos(\phi_{\bar{A}}) + j S_{\bar{A}} \sin(\phi_{\bar{A}})$ $ S_{\bar{A}} $ $20 \text{ LOG}_{10} S_{\bar{A}} $ $\phi_{\bar{A}}$ $ S_{\bar{A}} \cos \phi_{\bar{A}}$ $ S_{\bar{A}} \sin \phi_{\bar{A}}$	Complex spectrum of the average time data. Magnitude S _A defines the spectral content. Phase angle φ _A describes relative phasing of periodic harmonic components. Absolute angles are only meaningful if analysis windows were synchronized to periodic harmonic data.
Probability Density Function (PDF)	$q(x) = \frac{d[Q(x)]}{dx} \text{ such that}$ $\int_a^b q(x) dx = P \left\{ a < A \leq b \right\}$	Statistic defining most probable amplitude of A(t).
Cumulative Distribution Function (CDF)	$Q(x) = P \left\{ A < x \right\} = \int_0^x q(x)$	Statistic defining probability that time signal A(t) has instantaneous amplitude of x or less.

Definition of Symbols

- A(t) - Input time function on Channel A
- B(t) - Input time function on Channel B
- |S| - Magnitude of instant FFT = $\sqrt{S_{REAL}^2 + S_{IMAG}^2}$
- φ - Phase angle of instant FFT = $\tan^{-1} \frac{S_{IMAG}}{S_{REAL}}$
- √-1
- S* - Complex conjugate of S = S_{REAL} - j S_{IMAG}
- (overbar) - Ensemble average
- t - Time
- τ - Artificially introduced time delay
- $\mathcal{F}\{ \}$ - Direct Fourier Transformation
- $\mathcal{F}^{-1}\{ \}$ - Inverse Fourier Transform

(Δ) Similar for Channel B

Table 5.1(b). Fast Fourier Transform Analyzer Display Functions (from Ref. 18)

TABLE 9-2 DEFINITIONS OF FUNCTIONS		
DISPLAY SELECT	FUNCTION COMPUTED	DESCRIPTION
Time (Δ) (Inpt. Time - IT)	$A(t)$	Digital time history of input signal. (Display shows actual data processed)
Instant FFT (Δ) (Inst. Spec. - IS)	$S_A = \mathcal{F}\{A(t)\}$ $= S_A \cos(\phi_A) + j S_A \sin(\phi_A)$	Complex spectrum of time history, $A(t)$. Magnitude $ S_A $ defines instantaneous spectral content. Phase angle, ϕ_A , describes <i>relative phasing</i> of periodic harmonic components. Absolute angles are only meaningful if analysis window is synchronized to periodic harmonic data.
LIN	$ S_A $	
LOG	$20 \text{ LOG}_{10} S_A $	
PHASE	ϕ_A	
REAL	$ S_A \cos \phi_A$	
IMAG	$ S_A \sin \phi_A$	
Aver. Spec. (Δ) (Pwr. Spec. - PS)	$G_{AA} = \frac{S_A \cdot S_A^*}{S_A^2}$ G_{AA}	Ensemble average of squared spectrum magnitude (formed by multiplying complex spectrum by its conjugate). A real (rather than complex) spectrum, defining <i>average power</i> at each frequency.
LIN	G_{AA}	
LOG	$10 \text{ LOG}_{10} G_{AA}$	
(RMS Spec. - RS)	$\sqrt{G_{AA}}$	
Aver Cross Spec (X Spec. - CS)	$G_{AB} = \frac{S_B \cdot S_A^*}{S_A S_B}$ $= S_A S_B \cos(\phi_B - \phi_A) + j S_A S_B \sin(\phi_B - \phi_A)$	Ensemble averaged complex product of spectrum, S_B , with conjugated spectrum, S_A^* . Indicates those frequencies where <i>both</i> $A(t)$ and $B(t)$ have content. Phase angles indicate <i>average phase difference</i> between signals at each frequency.
LIN MAG	$ G_{AB} $	
LOG MAG	$10 \text{ LOG}_{10} G_{AB} $	
PHASE	$\phi_B - \phi_A$	
REAL	$ G_{AB} \cos(\phi_B - \phi_A)$	
IMAG	$ G_{AB} \sin(\phi_B - \phi_A)$	
Transfer Function (TF)	$H_{AB} = \frac{G_{AB}}{G_{AA}}$ $= \frac{ G_{AB} }{ G_{AA} } \cos(\phi_B - \phi_A) + j \frac{ G_{AB} }{ G_{AA} } \sin(\phi_B - \phi_A)$	Complex ratio of cross spectrum, G_{AB} , to input power spectrum, G_{AA} , defines the gain and phase lag introduced by a transmission system <i>excited</i> by $A(t)$ and <i>responding</i> with $B(t)$.
LIN MAG	$ H_{AB} $	
LOG MAG	$20 \text{ LOG}_{10} H_{AB} $	
PHASE	$\phi_B - \phi_A$	
REAL	$ H_{AB} \cos(\phi_B - \phi_A)$	
IMAG	$ H_{AB} \sin(\phi_B - \phi_A)$	
Transmissibility (TM)	$H'_{AB} = \frac{G_{BB}}{G_{AA}}$	Real ratio of output power spectrum to input power spectrum.
LIN	$ H'_{AB} $	
LOG	$20 \text{ LOG}_{10} H'_{AB} $	
Impulse Response (Imp. Resp. - IR)	$IR = \mathcal{F}^{-1}\{H_{AB}\}$	Impulse response of the system assuming input $A(t)$ and response $B(t)$.

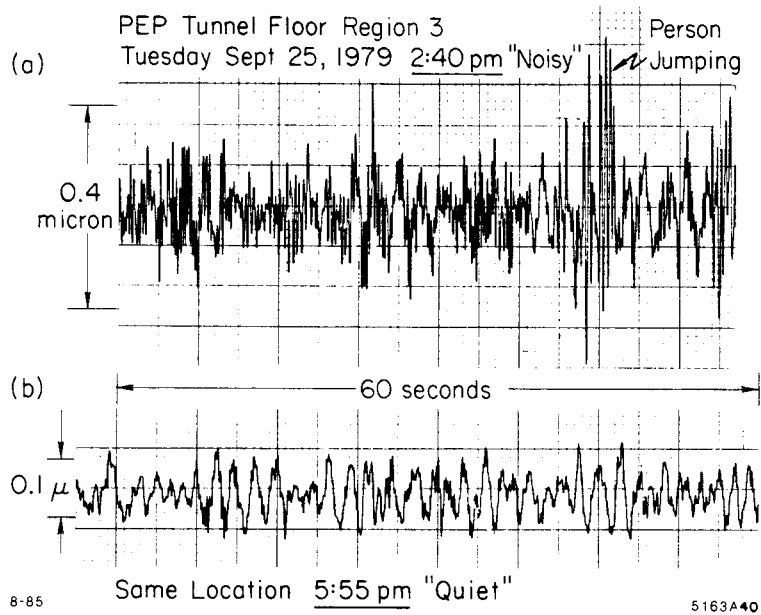


Fig. 5.2. "Raw Amplitude" Related Ground Noise Signal.

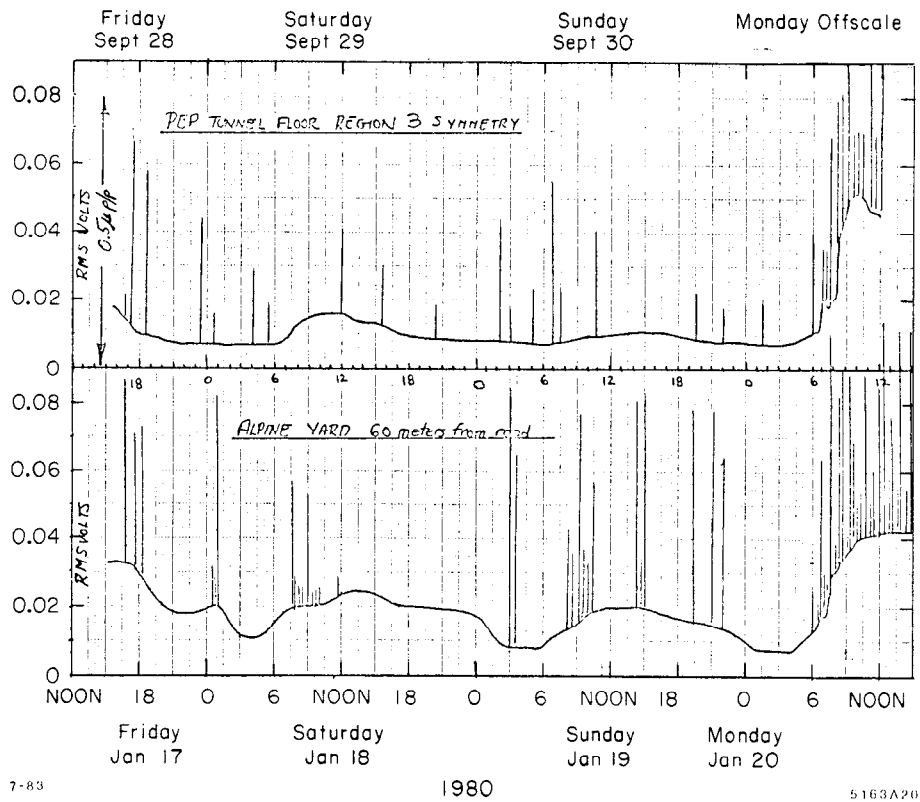


Fig. 5.3. R M S Base Levels and Transient Disturbances.

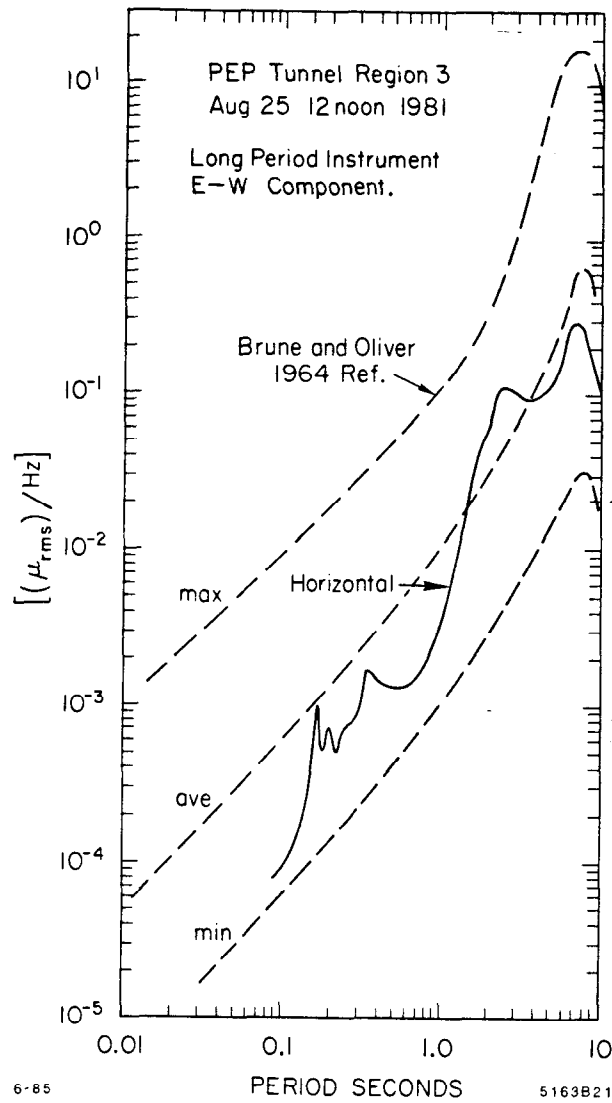


Fig. 5.3.1. Typical Noise Spectrum Measured in PEP Tunnel 100 feet Below Surface (Long Period East-West Component).

5.2.2 Transient Disturbances:

Most of the transient peaks in Figs. 5.3(a) and 5.3(b) are associated with either construction activity or *traffic*. To be somewhat more quantitative, we plot in Figs. 5.4 and 5.5 the total typical number of events having a peak amplitude greater than some number in a 6 hour interval as a function of time of day in the horizontal and vertical direction. The correlation with human activity is pretty clear. The sensors were on the surface in a not particularly well traveled area. Their location, I believe, is representative of a tunnel since we see from Fig. 5.3 that such transient disturbances are not much attenuated over distances of several hundred yards. Typical number versus amplitude plots are shown in Fig. 5.6. Vertical disturbances dominate – not inconsistent with traffic.

While these studies were underway, two anomalous transient events occurred. While they have nothing to do with the subject under discussion here, they are nevertheless instructive.

One day the Synchrotron Radiation Laboratory, which has been bothered by ground shaking since their photon beam lines have very long lever arms, called up to ask if the digging of the damping ring vault 2 miles away could be disturbing their experiments. We set up the instruments to monitor the construction activity and saw no effect. But, on Sunday night, May 24, 1981, at 22:53:37 hours, the recorder picked up a significant motion lasting 3 minutes. At 23:16 hrs. a rolling motion of a 20-second period began, lasting for another hour. See Fig. 5.7. The explanation came the next day when a magnitude 7.3 on the Richter scale earthquake was announced in New Zealand, Fig. 5.8. Using coordinates listed, one can reconstruct that the first disturbance seen must have been a direct s wave, flight time about 26 minutes, and the later motion the arrival of long period Love and Rayleigh Waves traveling in the crust of the Pacific Ocean floor with a flight time of 42-47 minutes. I was thrilled to have received a message from 12000 km away without the use of electromagnetism. Figure 5.9 depicts the geometric situation and core velocities are shown in Fig. 5.10.

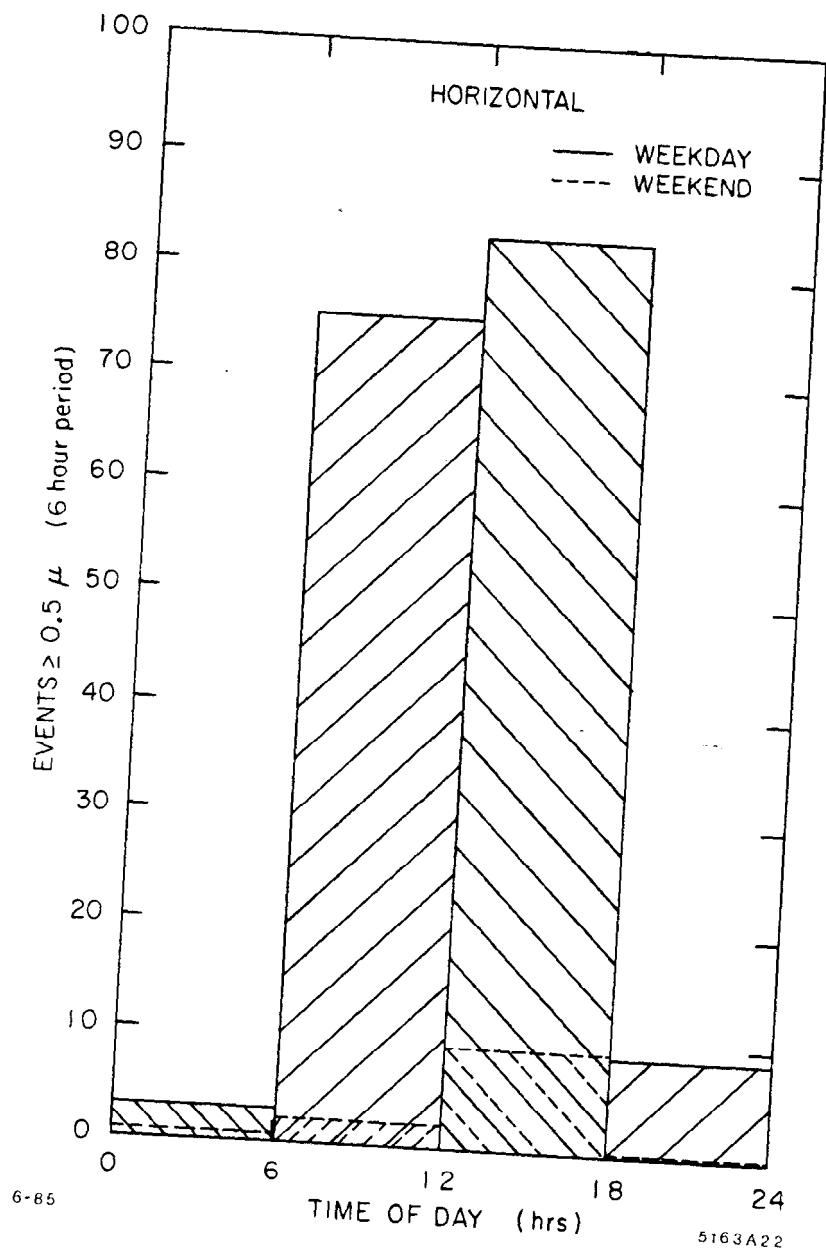


Fig. 5.4. Number of Horizontal Transient Events/6 hour Interval as a Function of Time of Day.

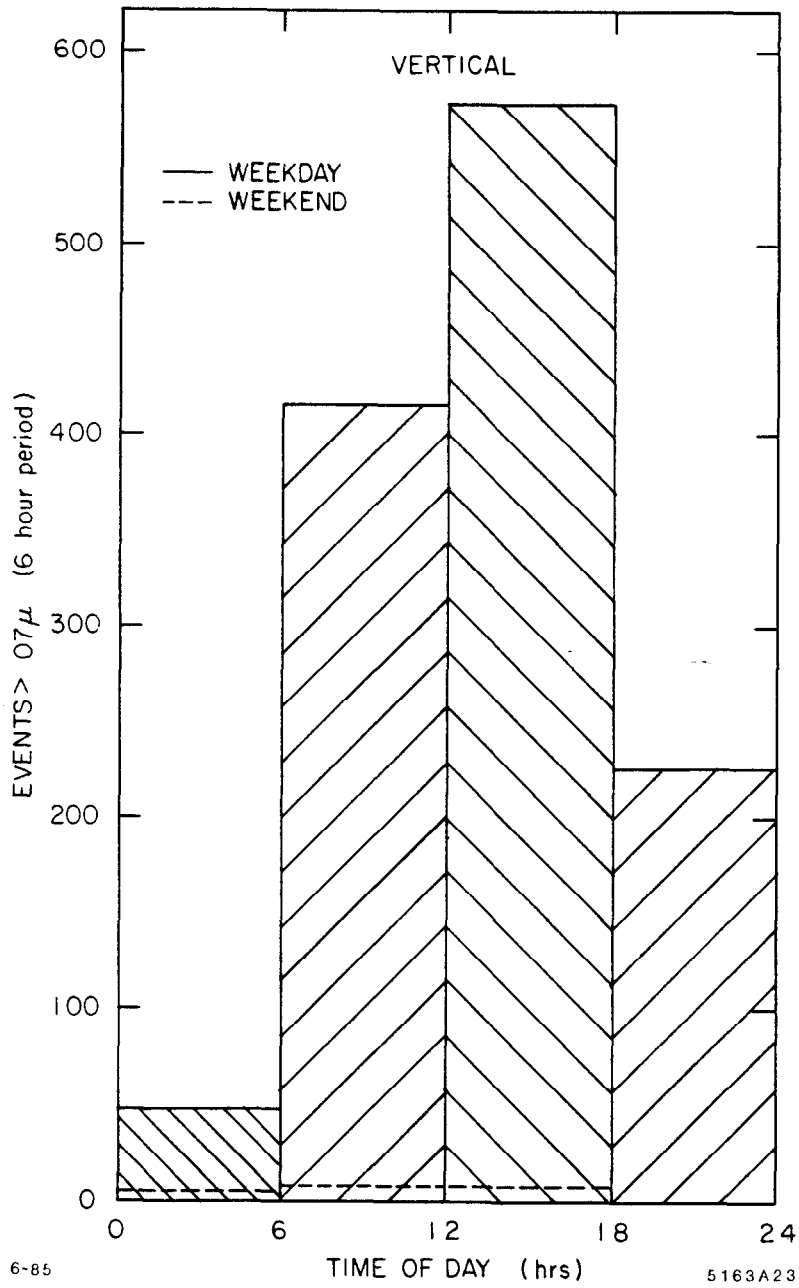


Fig. 5.5. Number of Vertical Transient Events/6 hour Interval as a Function of Time of Day.

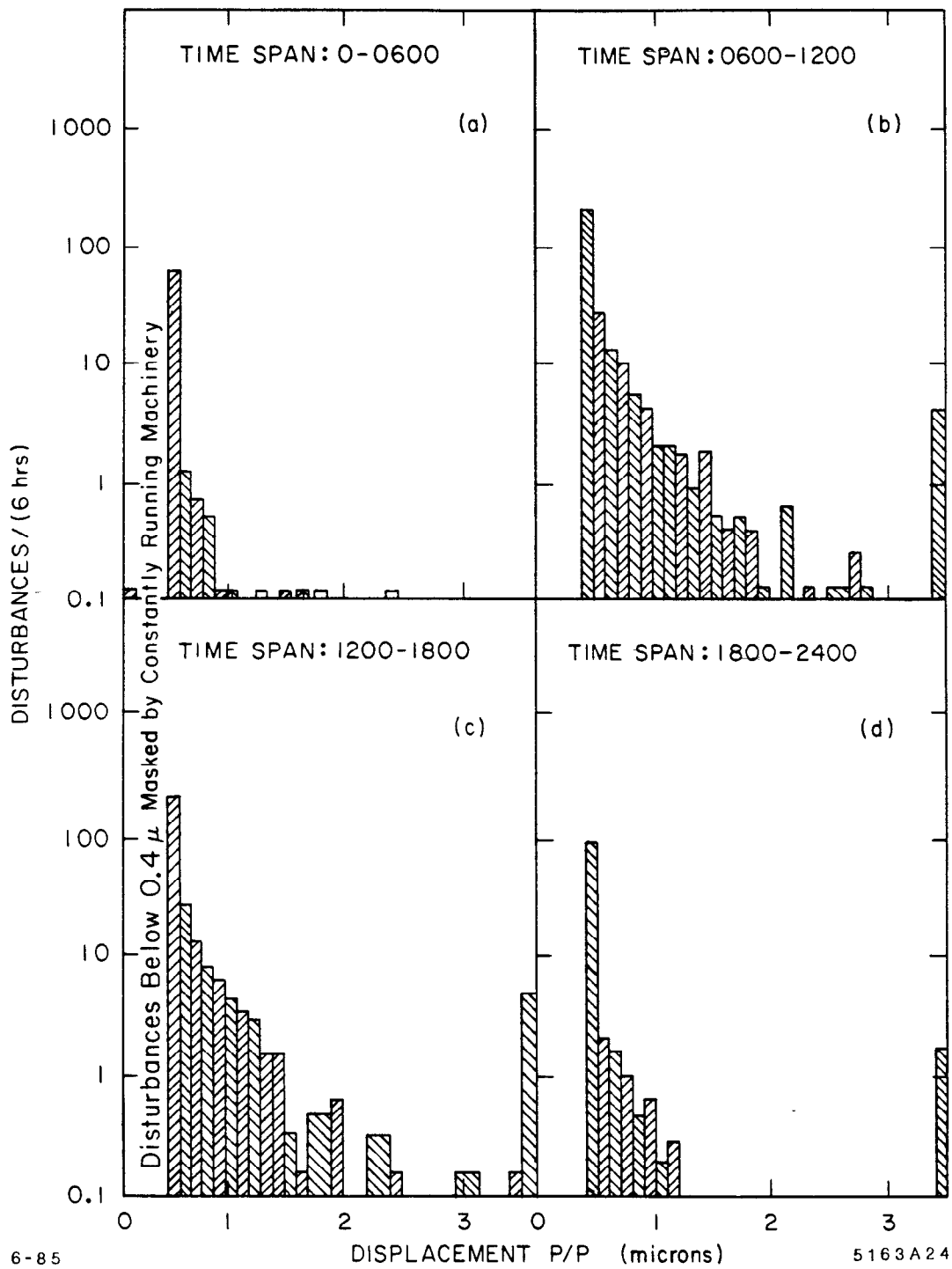
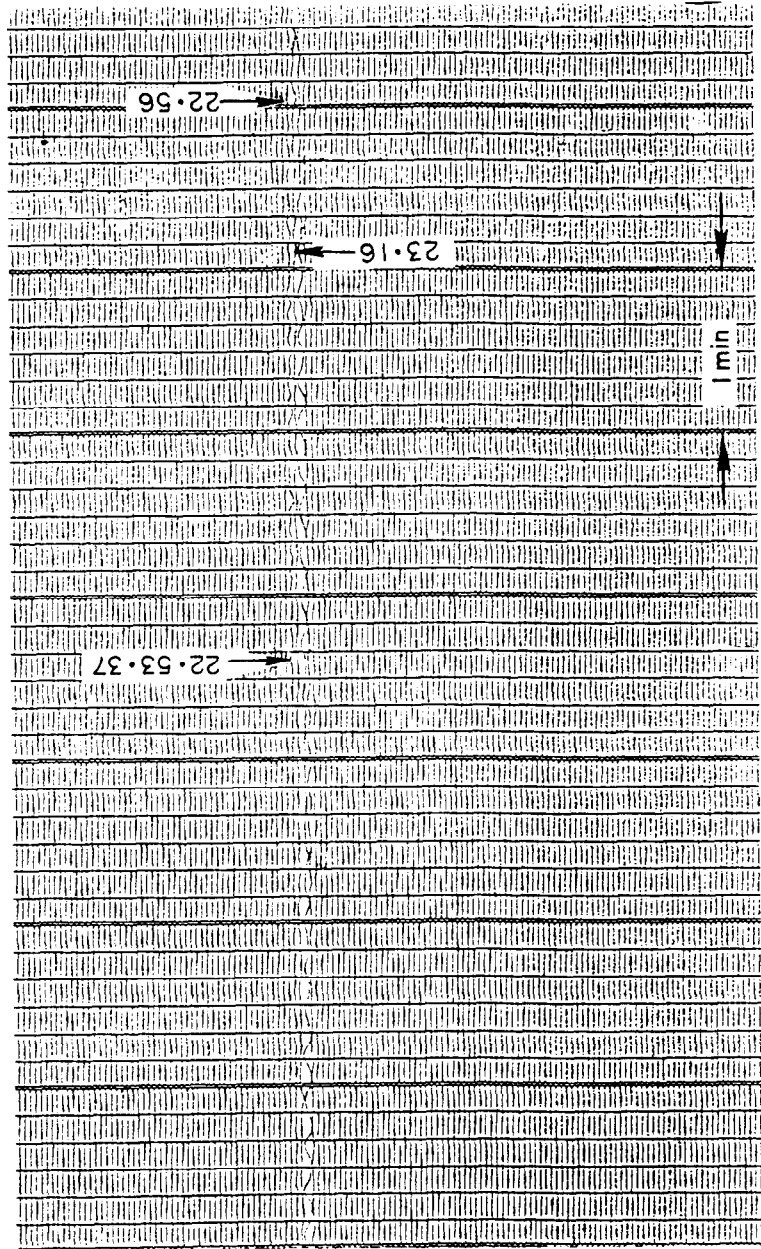


Fig. 5.6. "Amplitude Spectrum" of Transient Signals.



5163A25

6-85

Fig. 5.7. An Anomalous Event - Long Period (20 Sec) Seismic Waves Lasting About 1½ Hours.

Major Earthquake In Pacific Ocean

Honolulu

An earthquake measuring 7.3 on the Richter scale was recorded in the Pacific Ocean southwest of New Zealand early yesterday, according to the Pacific Tsunami Warning Center in Honolulu.

The earthquake, which occurred at 5:25 p.m., New Zealand time, was located in an area between New Zealand and the Auckland Islands, said Gordon Burton, a spokesman for the center.

"It probably didn't do much damage because there's no land in the area, but I'm sure they felt it in New Zealand," Burton said.

He put the exact location of the earthquake at 49.3 degrees south latitude and 164.7 degrees east longitude.

The quake was not expected to generate any tsunamis, or tidal waves, in the Pacific area, he said.

The U.S. Geological Survey in Washington said preliminary estimates put the magnitude of the quake at 7.5 on the Richter scale. A USGS spokesman, Don Kelly, said it appeared to be the largest quake since the magnitude 7.7 quake in Algeria last October 10.

Associated Press

6-85

5163A26

Fig. 5.8. Explanation of the Event Shown in Fig. 5.7 (from S. F. Chronicle).

Seismic wave travel paths through the earth. The time in minutes it took each wave to travel from the earthquake is shown where the paths surface. Over a little less than half the earth, directly opposite the earthquake focus, there are no direct, unreflected S wave arrivals. Note the reflected P wave (15.2 min) and S wave (27.3 min), in which the seismic energy bounced from the surface back into the interior. The paths are curved because of the increase of seismic velocity with depth within the earth.

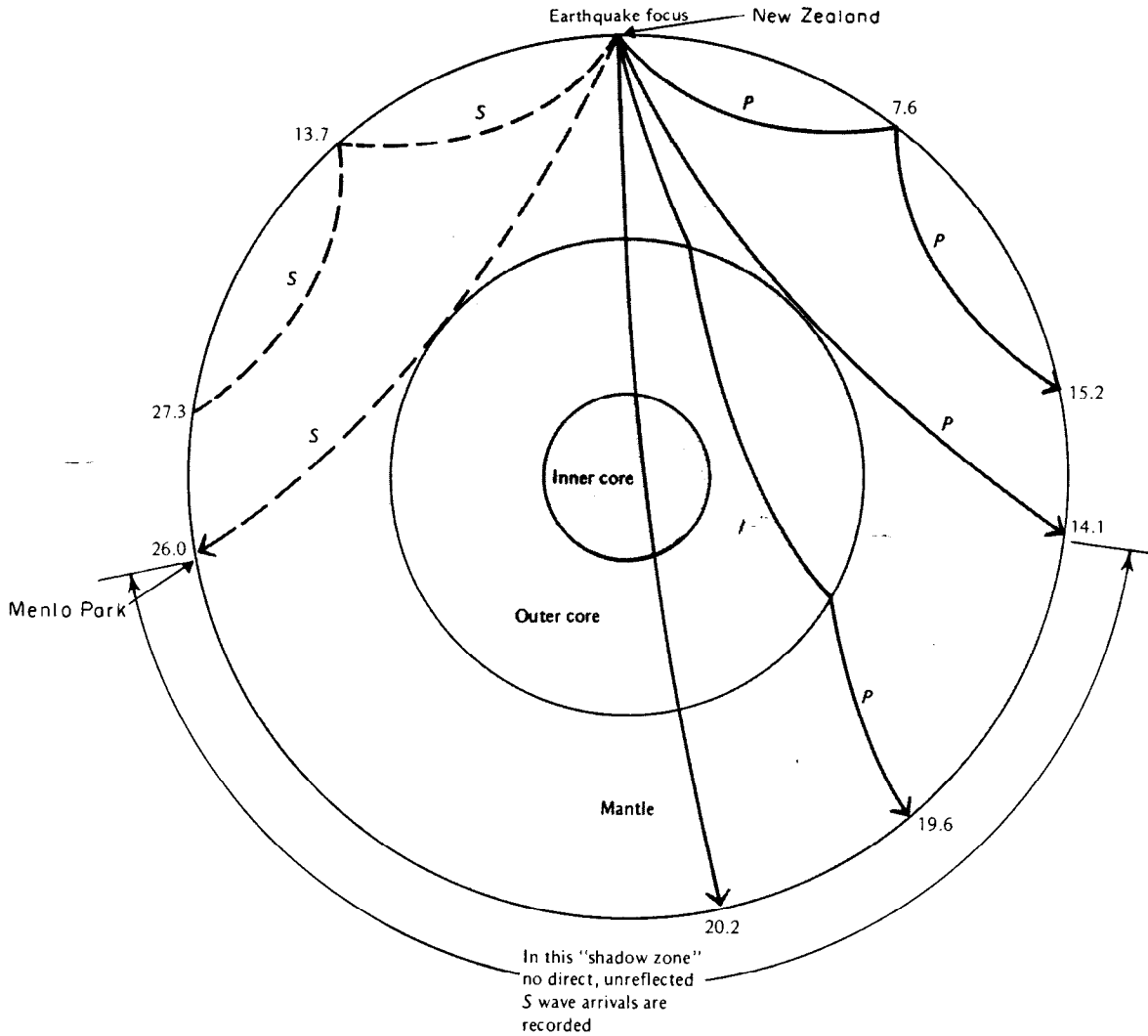
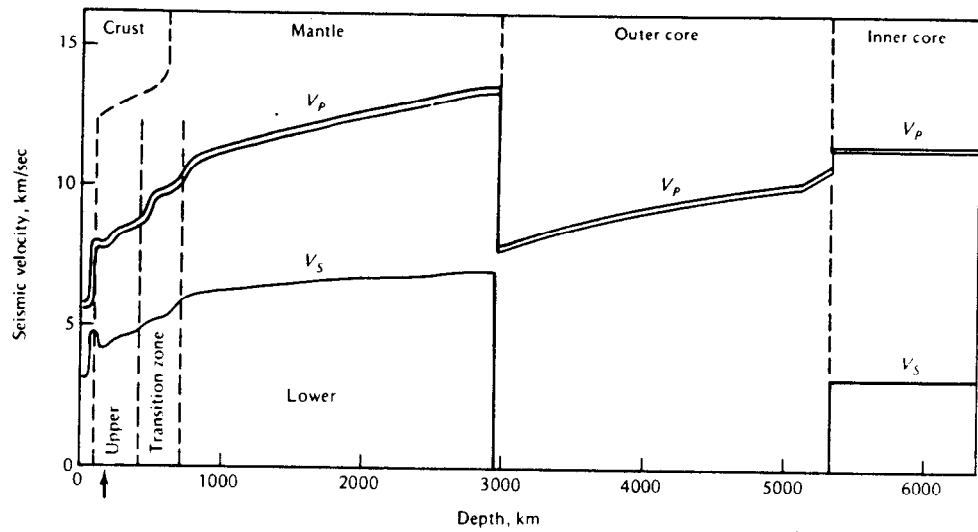


Fig. 5.9. Geometry and Arrival Times of Seismic Propagation (New Zealand to Menlo Park, California) (from Ref. 3).

The variation of seismic velocity with depth within the earth; v_p is compressional (P wave) velocity, and v_s is the shear (S) wave velocity. Note that the S wave velocity drops to zero in the outer core. The velocities for the inner core are somewhat speculative. The region of low velocities, near 100-km depth, is called the seismic low velocity zone (colored arrow).



Approximate variation of density with depth within the earth. The density of the inner core is not well known. Note the inversion of density—heavier material on top of lighter—at about 100-km depth.

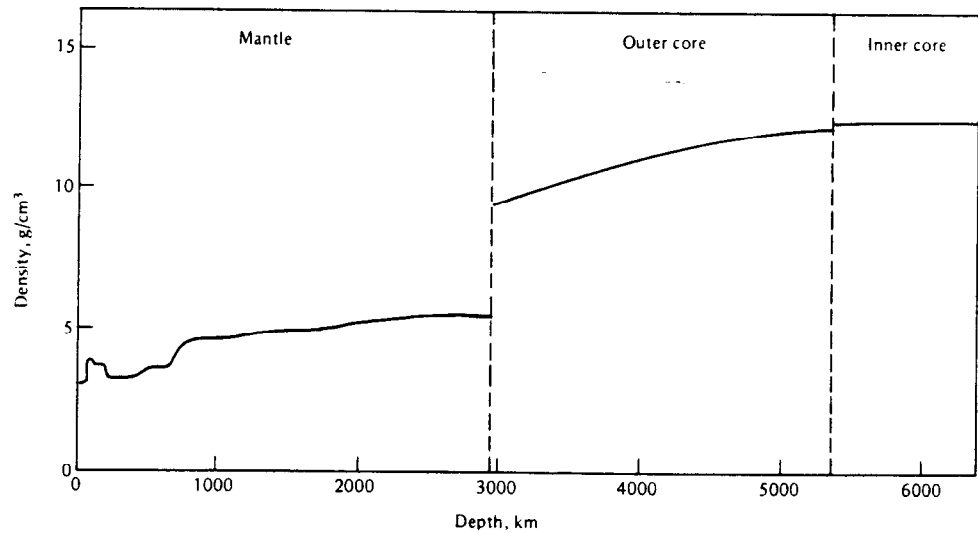


Fig. 5.10. Seismic Velocities in the Earth's Core (from Ref. 3).

Another event closer to home is shown in Fig. 5.11 – an earthquake and its aftershock in Coalinga, California. The clearly depicted difference in arrival time between the p and s waves is 26 seconds, consistent with a source to observer distance of 230 km. Amateur seismology in action!

As previously stated, earthquakes are rare and we should not be concerned with them in this context.

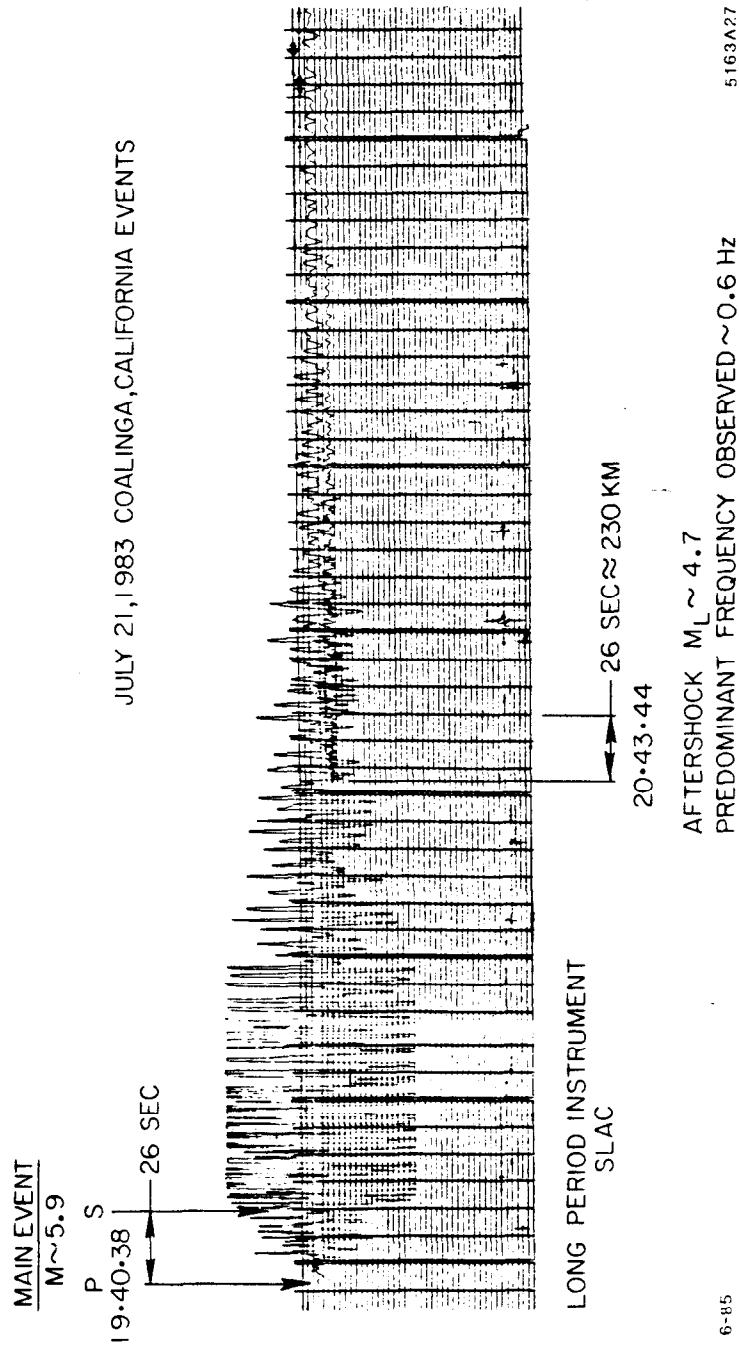


Fig. 5.11. Arrival of "p" and "s" Waves from a Recent Earthquake (Epicenter Coalinga, California).

5.2.3 Traffic

Since traffic disturbances appear to dominate transient noise, it was decided to investigate it further. A not unexpected result was that the size of the vehicle, its velocity and the condition of the road were parameters. The transient noise a vehicle traveling at 30-40 mph makes appears to be in the center of the frequency band 10 to 30 Hz and lasts for 3 to 15 seconds as it goes by. After a while we noticed that the various types of vehicles had characteristic frequency signatures. In fact, one could tell the difference between the Santa Clara and San Mateo county transit buses, the latter displaying a fairly sharp peak around 12 Hz when accelerating up a steep grade. A stop light does wonders. Little energy appears to be transferred to the ground in braking to a stop.

5.2.4 Continuously Operating Machines

Large fans, water pumps, water surging in cooling pipes, because they operate in the steady state, contribute to the general level of site noise. The severest offenders are heavy (say > 20 Hp) low frequency reciprocating devices such as vacuum pumps, air, helium or hydrogen compressors and, of course, bubble chambers. Their noise shows up all over the site on the ground spectrum as sharp well-defined spectral lines. Because their signatures are clean and ever present, the detective work of finding them as sources is relatively straightforward. We believe that the major offenders at SLAC have been located.

5.2.5 Detector Assembly Activity

The question: *Can a detector be assembled next to an operating linear collider?* appears in the light of what has already been said to have a rather surprising answer – perhaps, yes.¹⁹ Studies have been carried out with a crane in a well engineered collider assembly hall. They show, if the rails are sufficiently smooth, that little noise is transferred to the ground even when moving heavy (20 ton) objects. Of course, when these object are set down with a bump, or the crane trolley is run against its limit stops, substantial transients (up to 1/2 mm) are observed. At a massive detector (3000 tons 50 feet away) the amplitudes were less than 10 microns. The transients are completely damped in less than a few seconds.

5.2.6 Relative Phase Measurements

The spatial as well as the temporal characteristics of ground motion are of interest when one attempts to evaluate orbit distortions resulting from time varying quadrupole displacements. In other words, one needs to know the spatial correlations of quad displacements along the orbit's path. A correlation with the betatron wavelength would be, for example, potentially more dangerous than from, say, purely statistically uncorrelated quad motions.

The space versus time relationship of ground motion is, of course, related by the *effective velocity* of sound in the supporting medium. The medium consists of the ground itself, the tunnel floor and the magnet support structure – the latter two having perhaps transmission line characteristics of their own. The question, therefore, is: What values of velocity should one use for the various types of disturbances that will be encountered in practice?

We have found it possible to measure the space correlations of the motion in the PEP tunnel with relatively simple apparatus.²⁰ Two vertically sensing geophones (A,B) of matched gain were connected to a two channel FFT (Nicolet 660) Analyzer used in the Transfer Function mode. See Fig. 5.12. in this mode the analyzer measures the complex ratio B/A of the Fourier transforms from which is derived the *relative phase angle* of the disturbances at any particular frequency within a selected band.

As a driving source we chose two 75 HP vertical piston air compressors whose sharp 6.00 Hz signal is ubiquitous over the site. Figure 5.13 depicts the geometry of the source in relation to observers in the PEP tunnel.

Test site #1 was chosen such that the time of arrival of, say, a cylindrically spreading wave train should be nearly independent of relative sensor separation in the tunnel. Test sites #2 and #3 are nearly in line with the direction of the propagation vector, albeit they are closer to the source.

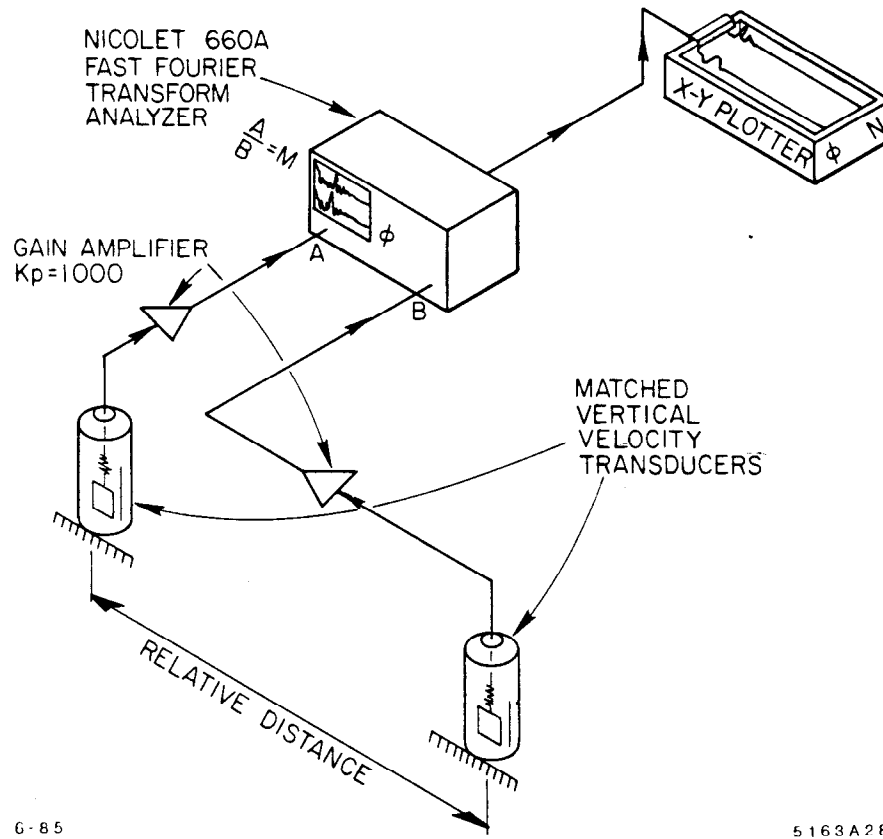
The data in Fig. 5.14 depict the relative phase angle between the signals from sensors A and B versus their physical separation in the tunnel.

As expected, there is little phase shift at PEP Region 3. In fact, although sensor A was geometrically slightly closer to the source, the signal arrived later than at B, indicating a velocity anomaly in the flight path – not altogether unlikely, since the terrain is quite inhomogeneous. The data from PEP Regions 1 and 11 show distinctive and almost linear slopes.

After translating sensor separation in the tunnel for line of travel geometry we can write, for the vertical amplitude:

$$Y(z, t) = Y_0 \sin(2\pi/\lambda)(z - vt)$$

EXPERIMENTAL SET-UP



G-85

5163A2B

Fig. 5.12. Experimental Set Up For the Detection Phase Differences.

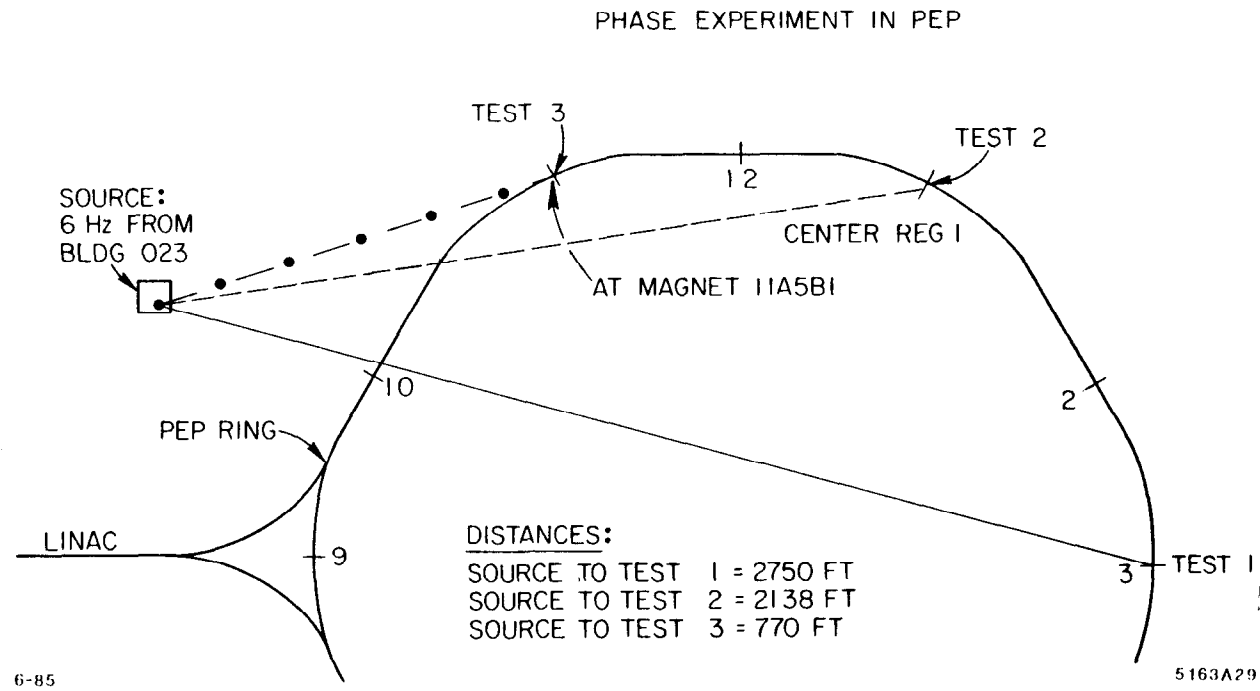


Fig. 5.13. Geometry for the Phase Shift Experiment.

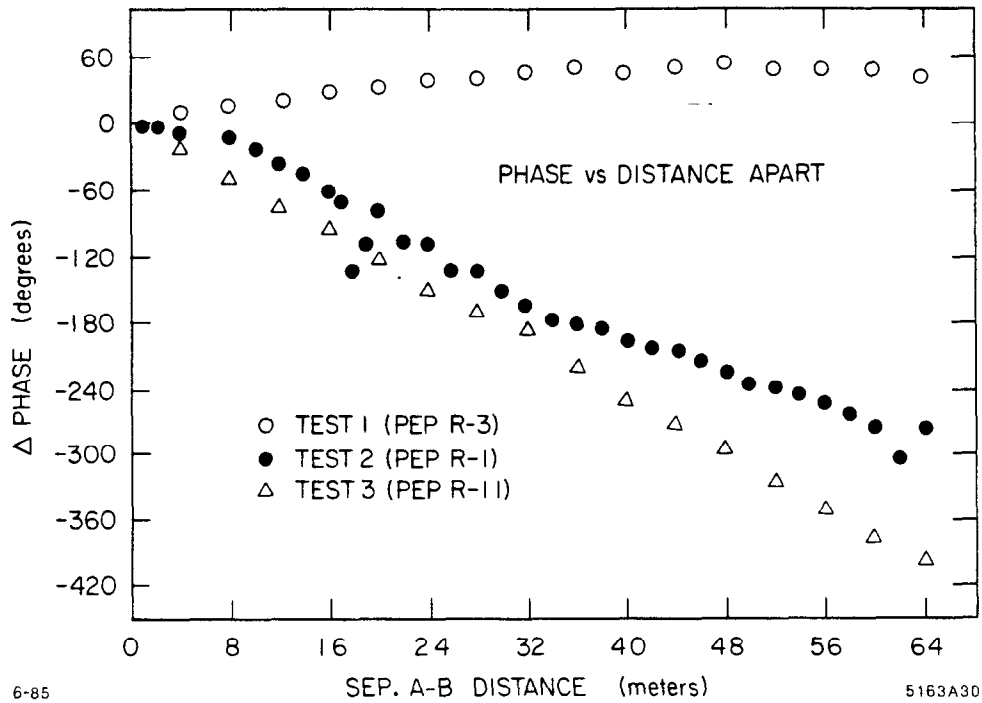


Fig. 5.14. Measured Phase Shift as a Function of Detector Separation.

then the local wavelength is:

$$\lambda = (z_1 - z_2) / (\phi_1 - \phi_2) \quad \phi \text{ in units of } 2\pi$$

and the local velocity of propagation is: $v = f * \lambda$, and obtain the following results:

Separation Between AB	Phase Shift	Proj. Dist.	Wave Length	Velocity ft/sec	km/sec	Depth Below Surface
Region 1 64 m	320°	157 ft	177 ft	1059	.32	16 ft
Region 11 64 m	397°	189 ft	171 ft	1028	.31	60 ft

Since both the source emitted and the sensors received in the vertical direction and the line of propagation is primarily in the horizontal, the velocities measured must be looked upon as *shear wave* velocities. If simple theory is valid, velocities should be frequency *independent*.

These results are not inconsistent with what might be expected in the *alluvial material* in the cut and cover Region 1, but it at first surprised us for Region 11 which is quite deep underground. An examination of bore hole data for Region 11 however showed that we had inadvertently picked a region which passes through layers of *clayey* and *sandy silts*.

On the other hand, it appears suspicious that the velocities in the two regions are so similar. We *may* be measuring the characteristics of the tunnel floor and not of the surrounding ground. A further experiment in a location of *known* more competent miocene sandstone would answer that question. In either case we are measuring a relevant quantity since the tunnel *floor* supports the magnets.

6. SOME GENERAL COMMENTS REGARDING LOCAL SOURCES

Up to now we have not discussed how the amplitudes of disturbances attenuate with distance from the source. There are two considerations: geometric wave spreading and attenuation properties of the transmitting medium.

6.1 GEOMETRIC SPREADING

If the dimensions of the problem are such that we can no longer consider the plane wave solution to the wave equation, then a different coordinate system is called for. Returning to the uniform, homogeneous isotropic and elastic medium discussed in Section 3.1, one can write for the amplitude of ground particle motion at distance from the source:

$$A_r/A_{r_0} = (r_0/r)$$

in which r_0 is sufficiently large compared to the dimensions of source that *near field* effects can be neglected., i.e., body waves spread spherically.

If the geometry of the problem is such that the motion is constrained to take place in a plane, then:

$$A_r/A_{r_0} = \sqrt{(r_0/r)} \quad \text{i.e., surface waves spread cylindrically.}$$

In the real world the situation is not so clear cut. The results of a simple experiment in a parking lot are shown in Fig. 6.1. In this situation a $1/r$ dependence appears not to have been too bad an approximation.

6.2 ATTENUATION WITHIN THE MEDIUM (INELASTICITY)

The solution to the wave question can also accommodate a term $\exp(-\alpha r)$ (α real) which is another way of saying that the index of refraction is now *complex*. That well cemented sandstone has a lower attenuation coefficient α from, say, sand in which the grains can rub against each other is not hard to believe nor is it difficult to imagine, therefore, that α is frequency dependent. Measurements in the laboratory and in the field show for wide class of materials that $\alpha(f)$ is *directly proportional to frequency*. For a substance as grossly anisotropic as shale, for example, of course the value of α_s for the shear wave is

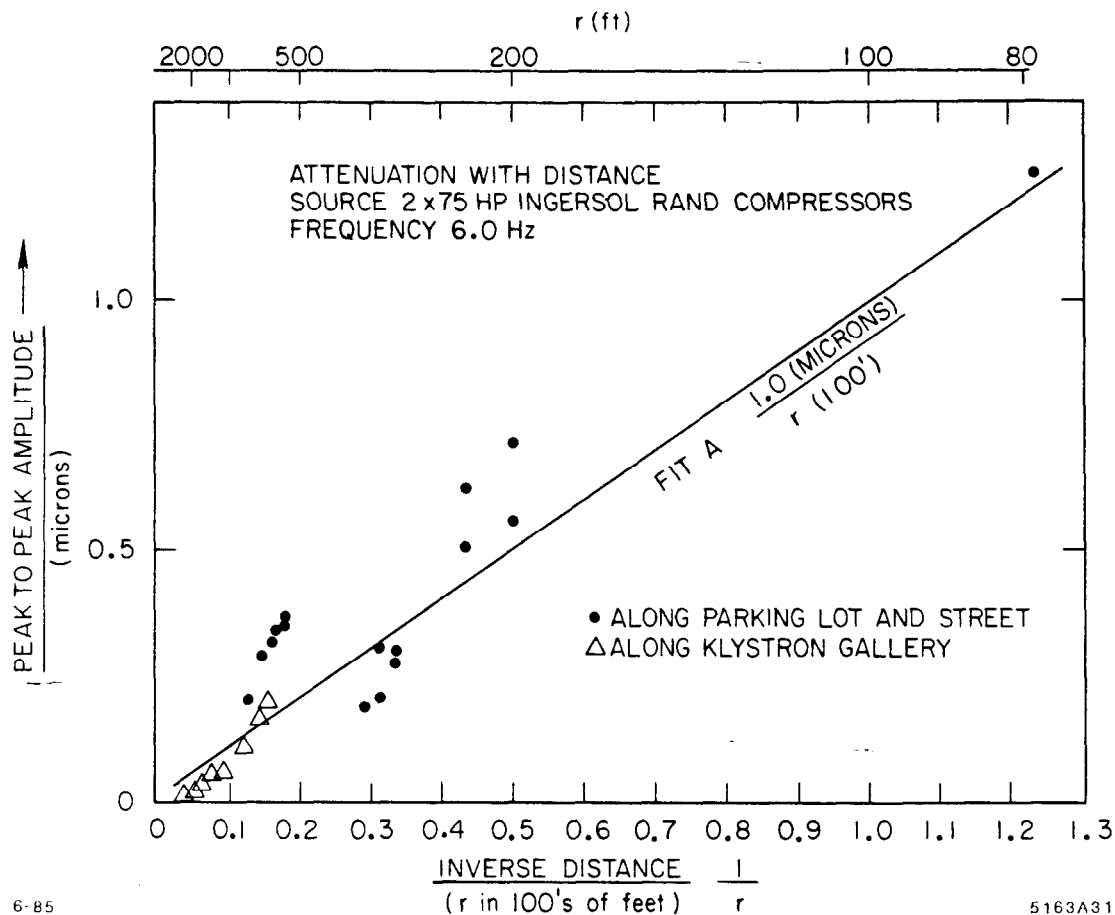


Fig. 6.1. Amplitude Signal Strength vs. Distance from a Local Source.

much higher than α_p for the p wave. Values of the loss parameter α expressed in units of f sec/cm are shown in Table 6.1.²¹

Often you will see the expression

$$A_r = \frac{A_o}{\sqrt{r/r_o}} \exp\{-\pi f r / c Q\} \quad \text{then} \quad 1/Q = \alpha c / \pi f = 2\delta f / f$$

in which c = velocity ,

f = frequency

α = attenuation/ l

δf = half width at .707 response

To provide a feeling for these quantities, let's plug in some numbers. For sandstone, using $\alpha = 3.5 \times 10^{-8} f$ sec/cm, a *plane wave* disturbance at 6 Hz would be attenuated in a flight path of 2 km by only about 4% - i.e., hardly at all. It also shows that disturbances from very distant earthquakes lose their high frequency

Table 6.1. Listing of Attenuation Constants of Various Materials (from Ref. 21)

MEASURED LOSS PARAMETERS FOR SEVERAL ROCK TYPES

Rock Type	c_p , km/sec	c_s , km/sec	θ_p	θ_s	θ_y	Frequency, cps	Loss Parameter Observed	Method	Ref.*
Granite: Sample 105	4.55	0.0064	1×10^4	$a_p = 0.044/\text{cm}$ at 10^4 cps	Multiple reflection of sine-wave train	68
Kamyk	6.1	3.5	0.0076	$(0.2-2) \times 10^4$	$a_p = 3.9 \times 10^{-5}/\text{sec/cm}$	Short pulse, direct path only	34, 65
Sample 3	5.50	3.30	0.048	0.035	0.040	$(30-180) \times 10^3$	$a_p = 27 \times 10^{-5}/\text{sec/cm}$ $a_s = 33 \times 10^{-5}/\text{sec/cm}$	Short pulse, 45° profile on block	62, 63
Sample 4	4.88	2.99	0.022	0.016	0.019	$(30-180) \times 10^3$	$a_p = 14 \times 10^{-5}/\text{sec/cm}$ $a_s = 17 \times 10^{-5}/\text{sec/cm}$	Short pulse, 45° profile on block	62, 63
Quincy	4.30	2.81	0.008	0.006	0.007	140-4,500	$Q_y = 100-200$; $c_y = 4.21$ km/sec $Q_s = 150-200$ $(\Delta W/W)_y = 0.1$	Long. resonance Torsional resonance Flexure of beam	6
Specimen Limestone: Solenhofen	0.016	40-120	10
Sample I-1	6.1	3.2	0.006	≈ 0.0024	0.0032	$(3-15) \times 10^4$	$a_p = 5.2 \times 10^{-5}/\text{sec/cm}$ $a_s = 5.8 \times 10^{-5}/\text{sec/cm}$ $a_y = 3.1 \times 10^{-5}/\text{sec/cm}$ $a_z = 2.5 \times 10^{-5}/\text{sec/cm}$	Multiple reflection of sine-wave train	53
Hunton Solenhofen	3.15	0.0016	0.015	$(3-10) \times 10^4$	$Q_y = 65$; $c_y = 4.0$ km/sec	Long. resonance	8
Solenhofen	3.1	0.0013	$(8-30) \times 10^4$ 5	$Q_s = 630$ $\delta_s = 0.004$	Torsional resonance Decaying oscillations of torsion pendulum	52 52
Shelly	0.016	40-120	$(\Delta W/W)_y = 0.1$	Flexure of beam	10
Shelly	0.003	10-40	$\theta_y = 0.003$	Flexure of beam	64
Sandstone: Sample 116	5.0	0.0056	1×10^4	$a_p = 0.035/\text{cm}$ at 10^4 cps	Multiple reflection of sine-wave train	68
Amherst	0.019	900-1,300	$Q_y = 52$; $c_y = 2.2$ km/sec	Long. resonance	8
Soft	0.048	40-120	$(\Delta W/W)_y = 0.3$	Flexure of beam	10
Old Red	0.011	10-40	$\theta_y = 0.011$	Flexure of beam	64
Chalk: Chislehurst	2.3	1.24	0.0007	0.0005	0.0005	600	$a_p \approx 6 \times 10^{-6}/\text{cm}$ at 600 cps $a_s \approx 7 \times 10^{-6}/\text{cm}$ at 600 cps	Bulk medium, sine-wave train	16
Shale: Sylvan	0.014	$(3-12) \times 10^4$	$Q_y = 70$; $c_y = 3.65$ km/sec	Long. resonance	8
Pierre	2.2	0.81	0.031	0.103	0.098	50-450 20-125	$a_p = 45 \times 10^{-5}/\text{sec/cm}$ $a_s = 4 \times 10^{-5}/\text{sec/cm}$	Bulk medium, Fourier analysis of pulses	44

* Numbers refer to entries in the bibliography at the end of this chapter.

information. Very long period Rayleigh waves in the earth's upper mantle are reported to have an $\alpha_R = 36 \times 10^{-9}/\text{cm}$ at a frequency of 7.1×10^{-3} Hz and $C_R = 4.2$ km/sec (N. Ewing and F. Press, 1954).²²

One should mention here, but only for completeness, that our treatment, although accommodating dispersion, has been in *linear* theory. Loss mechanisms can be, in fact mostly are, profoundly hysteretic, i.e., nonlinear in amplitude. Since the amplitudes we are dealing with are very small, non-linear effects will not play a significant role.

6.3 MORE ON VELOCITIES IN THE GROUND

Throughout all of the preceding discussion we have harped on the role of knowing the appropriate velocities in the problem. For local disturbances local velocities are required. A typical depth profile for SLC tunnel routings calculated before the digging began by professionals on the basis of bore hole and seismic surveys is shown in Fig. 6.2. Figure 6.3 displays velocity results in this particular region. Just to show you that my interests are not completely parochial, cut *C'C* of Fig. 6.4 shows the material in a deep section through the American continent not far from where Fermilab is located.

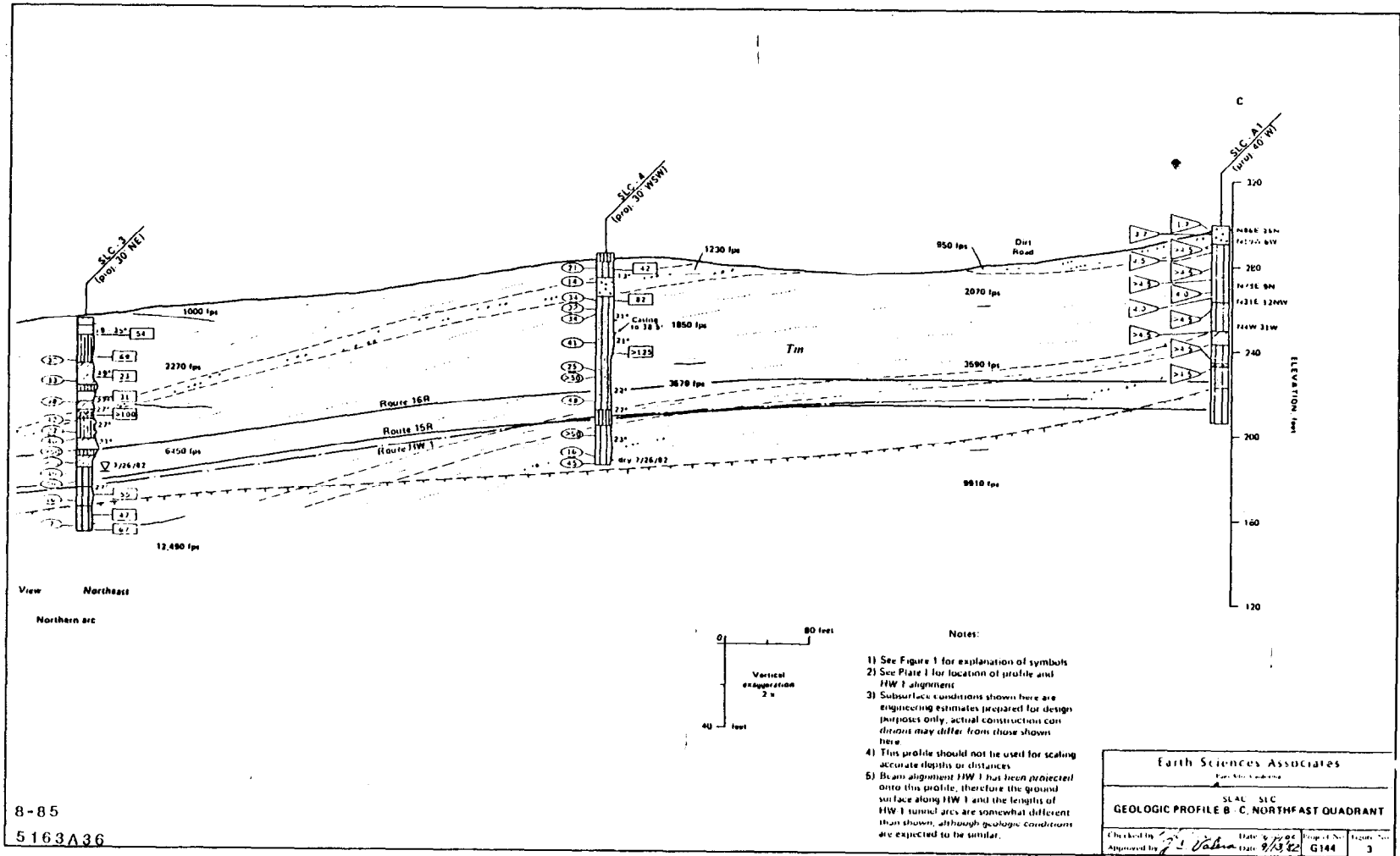


Fig. 6.2. Local Velocity Profile vs. Depth Derived from Bore Hole Logs used in Planning Tunnel Route in a Region of the SLC (from Earth Sciences Assoc. Palo Alto Report, September 1982).

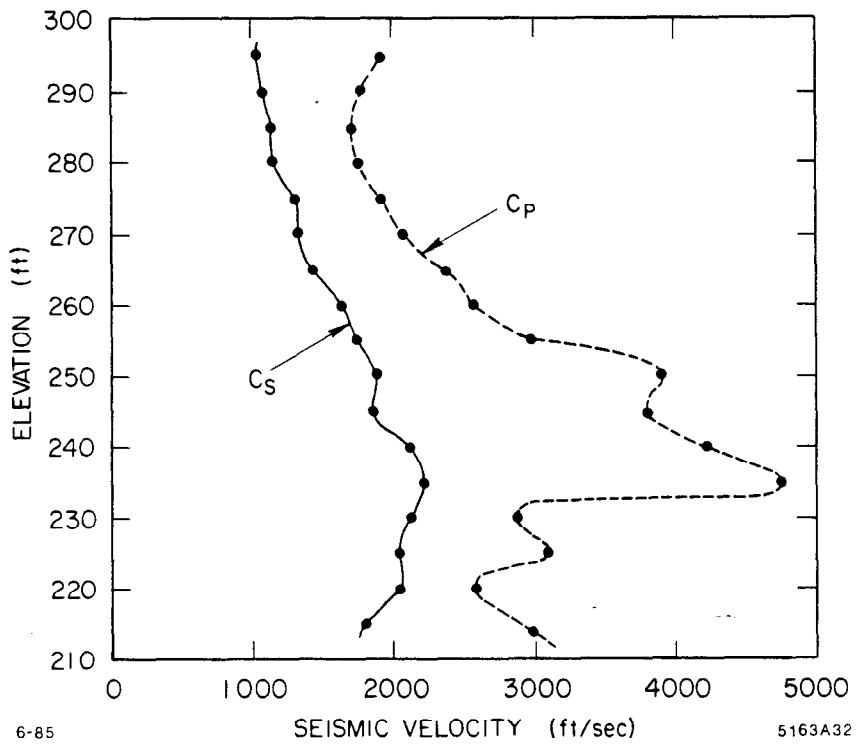


Fig. 6.3. Results of a Typical Seismic Survey.

Central stable region of United States. The contour lines on map represent the depth to the surface of the underlying basement rocks in feet. Note series of broad domes, arches and basins indicated by these contour lines. Lines A-A', B-B' and C-C' indicate geographic position of sections shown in Figure 8-28.

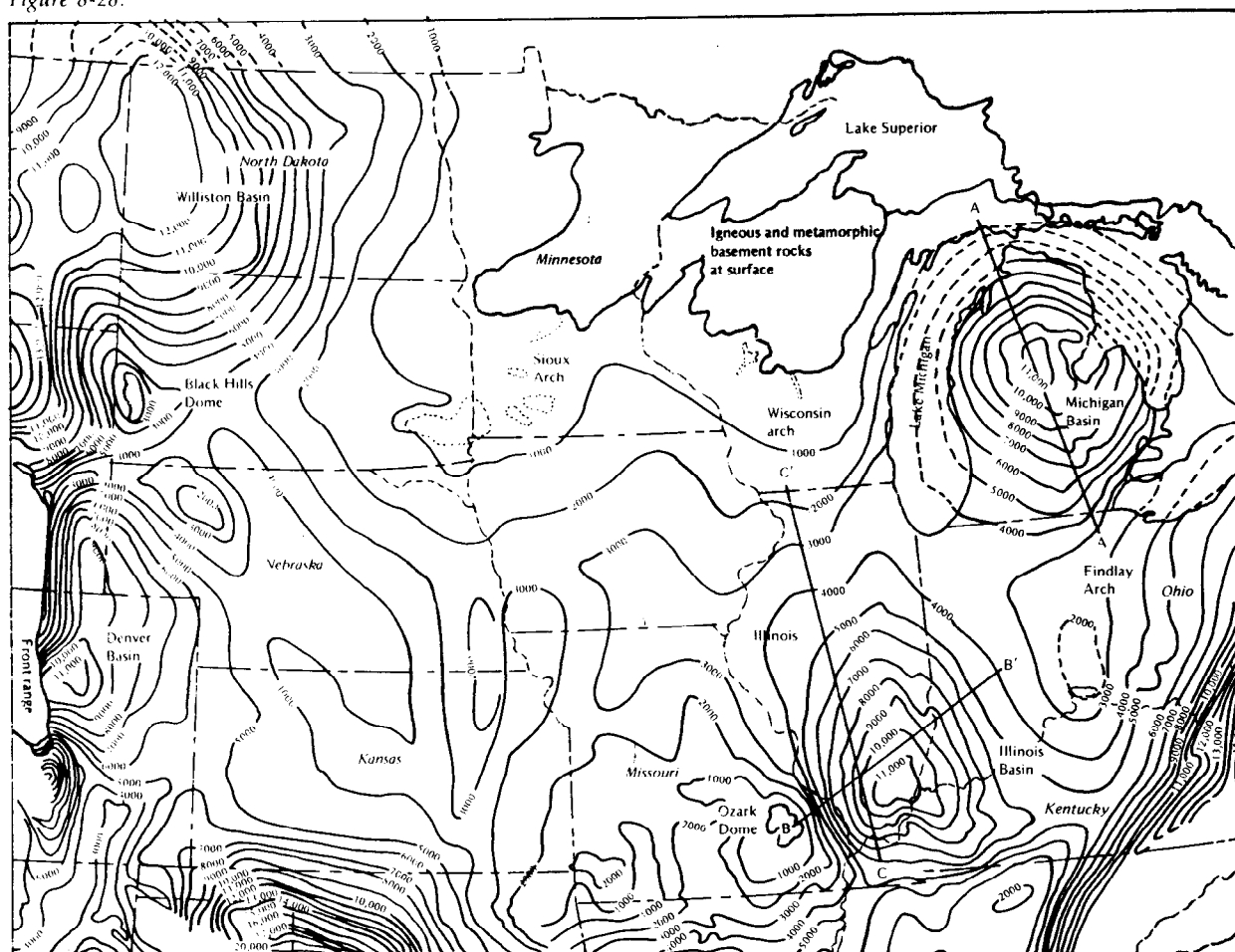
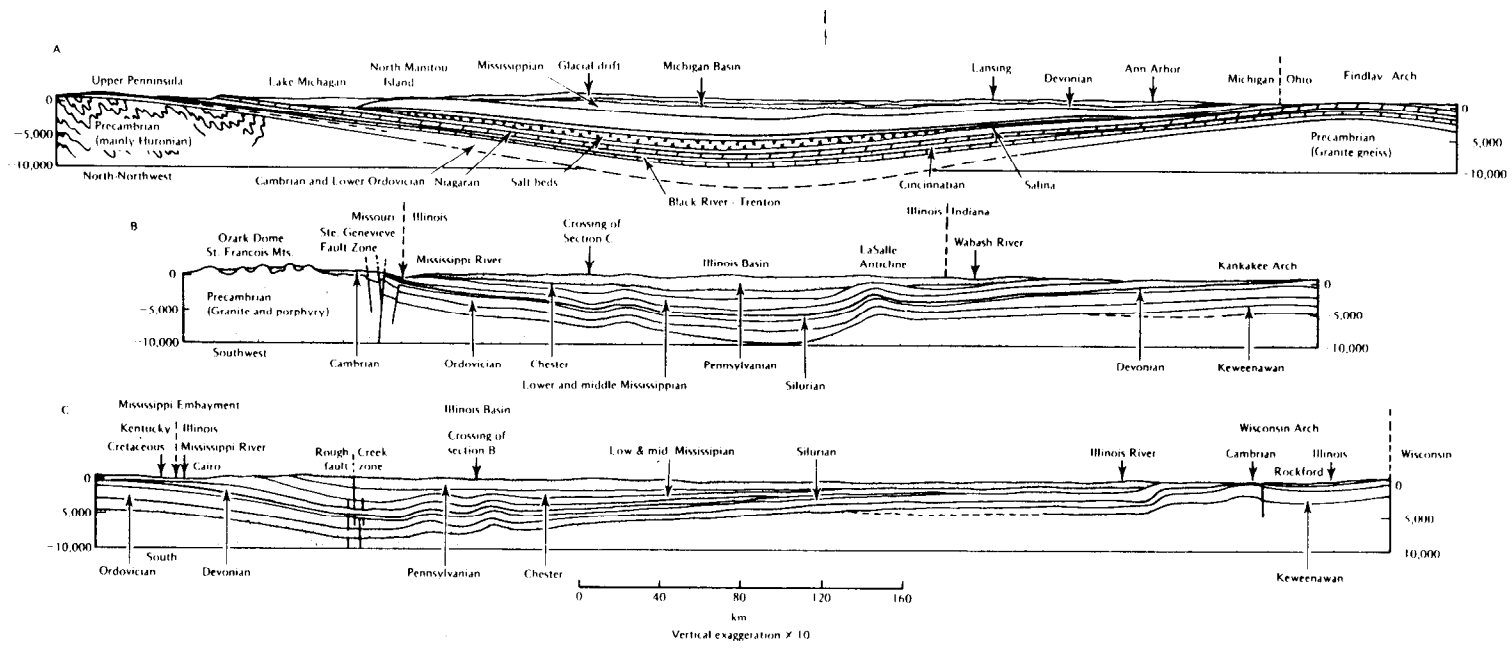


Fig. 6.4(a). Deep Underlying Strata in the Continental United States Near Fermilab (from Ref. 3).



Cross section showing stratigraphic relations of thin sedimentary units that cover the stable interior of the United States. Note gentle warping of basement surface and very gradual change in thickness of sedimentary units. Vertical exaggeration $\times 10$. The lines A-A', B-B', C-C', along which the sections have been constructed are shown in Figure 8-29. [From Phillip B. King: *The Tectonics of Middle North America*. Princeton University Press, Princeton, N.J., (p. 40, 1951). Used with permission.]

Fig. 6.4(b). Deep Underlying Strata in the Continental United States Near Fermilab (from Ref. 3).

7. WHAT TO DO ABOUT THE PROBLEM

Assuming for the moment that we *have* a problem, in this section we list some common sense counter measures that spring to mind.

7.1 NATURAL SITE CONSIDERATIONS

One would imagine it best not to build some large future machine next to Niagara Falls or directly on a seacoast subject to violent storms nor directly inside or too near a center of heavy industrialization or population. The underlying geology should be *competent* yet not so hard that you cannot easily cut or mine through it.

7.2 MITIGATION OF SOURCES

Heavy low frequency sources such as continuously operating reciprocating machinery can be: (1) moved to a distance at which their effect on the beam is negligible; (2) replaced with well balanced high rpm machines; (3) vibration isolated. In fact, there exists a whole *industry* dedicated to vibration isolation in which clever combinations of masses, platforms, springs and damping mechanisms are employed to prevent vibrational energy of being coupled to the ground. (See Ref. 23). Since heavy machinery is a necessity, and since its use spans all disciplines and functions of any laboratory, it behooves *laboratory management* to promulgate a *site-wide policy* regarding design review, installation and use - preferably before, rather than after, the fact.

Traffic is a matter not as easily dealt with but, as implied earlier, good roads, speed limits or stop signs do wonders.

7.3 COMPONENT AND COMPONENT SUPPORT DESIGN

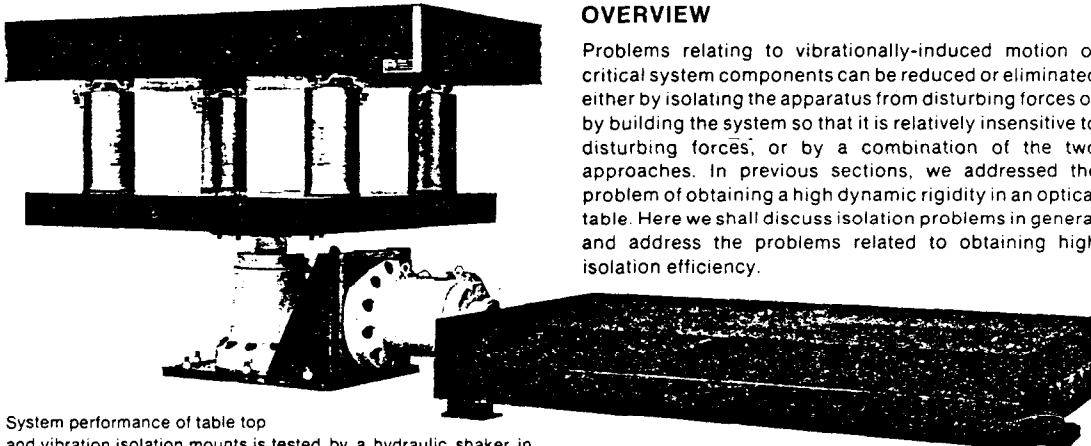
As is well known, turbulent water flow in supply pipes, magnet coils or beam collimators can shake critical components. Unfortunately the desires, to keep heat transfer coefficients high and water turbulence (i.e., velocity) low, are contradictory. Careful engineering compromises must be made.

Just, as in the case of isolating sources from coupling *to* the ground, there exists a whole industry of isolating critical components *from* ground motion. Notable is the application of these principles to laser optical systems used in large scale holography. In this case the relative motion of elements must be controlled to fractions of a wavelength of light. A typical system, employing hydraulically activated legs, is shown in Fig. 7.1.²⁴ Since it is generally more economic to shield the source rather than the receiver, such ideas are probably best limited to super-critical components such as "high-beta" interaction region quadrupoles if all other counter measures fail. Still, all component support designs should be analyzed for their dynamic mechanical response.

VIBRATION ISOLATION

OVERVIEW

Problems relating to vibrationally-induced motion of critical system components can be reduced or eliminated either by isolating the apparatus from disturbing forces or by building the system so that it is relatively insensitive to disturbing forces, or by a combination of the two approaches. In previous sections, we addressed the problem of obtaining a high dynamic rigidity in an optical table. Here we shall discuss isolation problems in general and address the problems related to obtaining high isolation efficiency.



System performance of table top and vibration isolation mounts is tested by a hydraulic shaker in both the vertical and the horizontal directions.

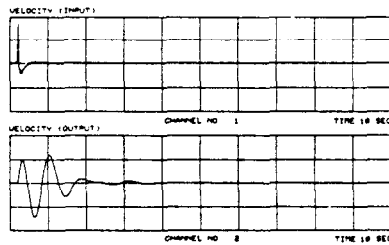


Fig. 13-1 - When excited by an impulse (above) using a hydraulic shaker, an RS512-12 table top that is supported by an XL4A-22 isolation system has a rapidly decaying vertical time response (bottom curve.)

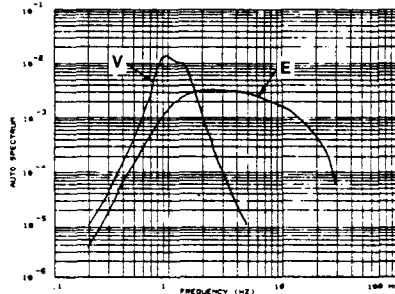


Fig. 13-2 - The frequency content, or autospectrum, of the air mount time response is shown for both the excitation impulse (E) and the vertical system response (V).

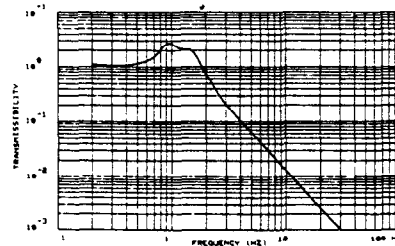


Fig. 13-3 - System vertical transmissibility, as a function of frequency, is obtained by dividing the air mount's output autospectrum by its input autospectrum, Fig. 13-2 above.

8-85



INTRODUCTION

Conventional isolation systems are passive and achieve their performance by behaving like soft springs. This is accomplished by using soft compliant materials such as rubber, composite pads, springs, or by using pneumatic systems. In contrast, active systems sense forces acting on the table or table motion and apply counteracting forces to null the system. To date, only a limited number of such systems have been built, and only for special applications at considerable expense.

The basic characteristic of a passive isolation system is its spring-like nature. For example, a table top that is supported by three or more isolation mounts is in effect a rigid body sitting on three or more soft springs. If we ignore for a moment the fact that such a system has six degrees of freedom with six associated rigid-body resonances, and consider only pure vertical motion, we observe that the system is analogous to a simple, single degree of freedom spring-mass system. The mass has a classical response to base motion, with amplification of the base motion at frequencies up to $\sqrt{2}$ times the system resonant frequencies and attenuation or isolation at driving frequencies above $\sqrt{2}f_n$. It is desirable from an isolation standpoint to make f_n as low as possible, since it not only moves the resonant peak to lower frequencies (which should have less effect on a table and associated apparatus), but greatly improves performance for all frequencies above resonance as well. The question of how low to make f_n involves what is required, what is achievable, and what tradeoffs are involved. Experience has shown that considerable floor motion occurs at frequencies as low as 2 to 4 Hz with most energy being between 5 and 30 Hz. This means that f_n should be on the order of 1 Hz and definitely below 2 or 3 Hz. This effectively rules out rubber or composite pads since their resonances typically fall right in the spectral region where floor motion is the greatest and as a result they act as an amplifier rather than as an isolator. Steel springs are impractical and seldom used for this type of application because of the large static deflection involved (about 10" for a 1-Hz system), lateral instabilities, and surge. This leaves the pneumatic system as the sole remaining alternative for this type of application.

5163A37

13

Fig. 7.1. Example of a Pneumatic Vibration Isolation System under Test (from Ref. 24).

7.3.1 Theoretical Analysis

Structural analysis can be treated analytically or by means of computer aided finite element numerical methods.²⁵ The former is important in the understanding of simple bodies such as bending beams etc., while the latter is practical in "real life" situations when the number of coupled equations and their boundary conditions become unmanageable.

7.3.2 Experimental Analysis

Rarely do intuitive mathematical models describe the actual physical structures the first time they are derived - unless the engineer has a great deal of practical experience in this field. Nor would one embark on the construction of a large project without comparing the mathematical model with as close a mockup of magnets and their supports as one can afford to build. In this endeavor one can work in either the time or frequency domains.

In the latter, the measurement of the complex transfer function of the structure by means of an FFT apparatus (previously described) is particularly useful. With such a device, the structure's modal frequencies and damping coefficients are readily evaluated. Figure 7.2 shows, for example, the vertical oscillation frequency of an SLC magnet, excited by random noise generated by stomping about.

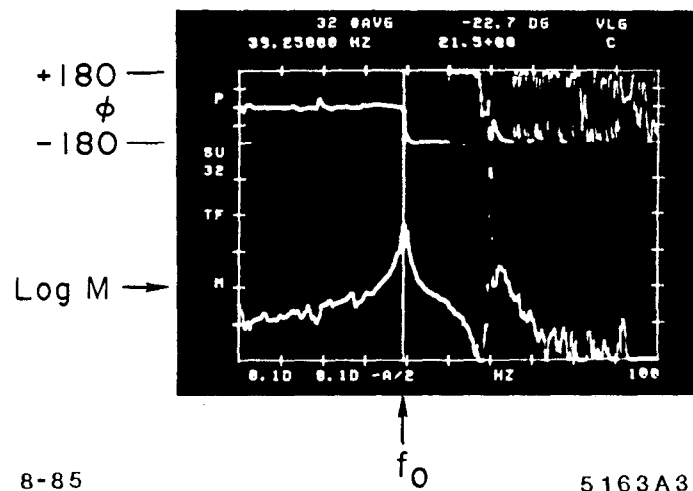


Fig. 7.2. Vertical Transfer Function of an SLC Alternate Gradient Magnet.

Note the classical phase shift as we pass through the resonance. If one used only one channel, all the many other vibrations in the building totally confuse the picture. In this example we observed that the Q of the magnet was amplitude dependent.

I suppose one should mention here some handy rules of thumb.

Consider a magnet of uniform cross section, w weight per unit length, and length L , simply supported at its ends (Fig. 7.3), which has been designed with a sectional modulus I such that it has a natural deflection under its own weight "d".

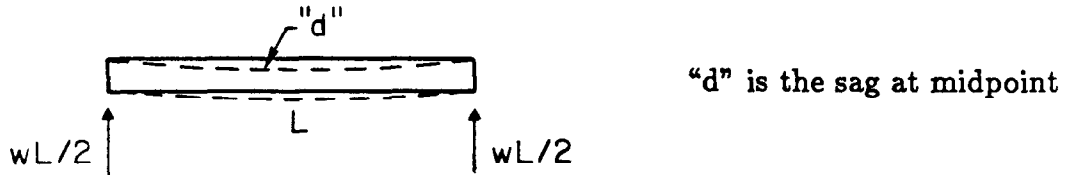


Fig. 7.3. A "Simply Supported" Bending Beam.

The natural vertical frequency of such a beam can be approximately written, (for modes $N = 1, 2, 3$ etc.) as:

$$f_N \text{ cycles/sec} = N^2 1.56 \sqrt{(gEI/wL^4)} \text{ in which } g = \text{acceleration due to gravity}$$

We see that these frequencies scale as $1/L^2$ and $1/\sqrt{w}$. Since the static deflection "d" is:

$$"d" = 5/385 (wL) L^3/EI$$

One can simply rewrite:

$$f_{cps} \approx N^2 1.56 \sqrt{(5/385)} \sqrt{(g/"d")} \approx 0.178 N^2 \sqrt{(g/"d")}$$

Exercise: Convince yourself that the above expressions are dimensionally correct.

Suppose now that we have some long object that would deflect a not unreasonable say 1/2 mm under its own weight. For the lowest mode ($N = 1$), $f = 25$ Hz – right in the middle of the traffic noise band. The next mode is at 100 Hz and therefore out of the noise. (This discussion demonstrates a little joke in the support fraternity, namely "everything around accelerators resonates at the wrong frequency.") If we cannot make the object stiffer, one can at least support it at its *quarter points* to push its frequency up out of harm's way.

To calculate the response of a system to some input forcing function, follow the procedure outlined in Fig. 3.4. In other words multiply together in turn the fourier transform of the forcing function with the fourier *transfer* – function of each element.

7.4 FEEDBACK ON BEAM DERIVED INFORMATION

In lecture 1 of this series Rae Stiening has already told you about feedback – therefore I shall not dwell on it here except to tell you that it is already being used with great success at the Stanford Synchrotron Radiation Laboratory (SSRL).

Experimenters, whose apparatus is located at the end of long (20 meter) photon beam lines, noticed for some time that the power density across their 2 mm high vertical slits was not constant. The secondary source of this problem was eventually traced back to the fact that the stored orbit was changing its direction of emission by minute ground motion induced *torsional* modes of most of the concrete girders that support the ring magnets.²⁶ The frequency of these modes (not the same on every girder) was centered about 4.5 Hz. The primary source of vibration was a hydrogen compressor located some 500 feet away and operating at 4.5 Hz.

In this case it proved to be expensive to isolate the primary source. Attempts to modify the torsional mode frequencies resulted only in shifting the beam error signal to other nearby frequencies. The solution was to increase the bandwidth of the *beam bump* steering system with which each photon line is equipped. The schematic of the system is shown in Fig. 7.4. The error signal is derived from a split anode helium ionization chamber located at the experimenters photon station.

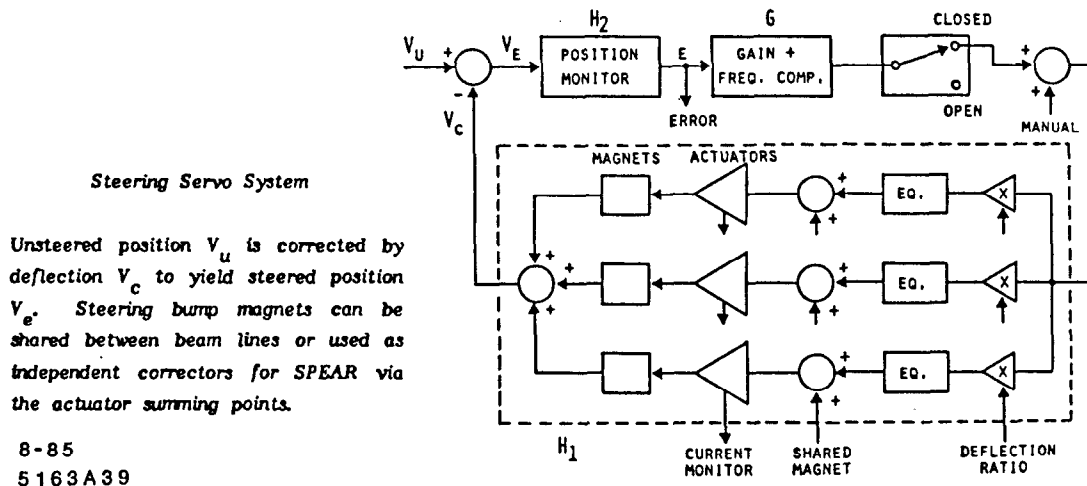


Fig. 7.4. Schematic of the SSRL "Beam Bump" Steering Feedback System (from Ref. 26).

A noise abatement factor of 36 db has been obtained but the system must be *tuned* manually to bring it into its operating range, and is probably bandwidth limited because the magnetic correcting fields are applied through the rather thick aluminum walls of the SPEAR vacuum chamber.

7.5 FEEDBACK/FEEDFORWARD ON SEISMIC ARRAY DERIVED INFORMATION

The system described above is not information limited by the sampling theorem because the circulation frequency in SPEAR is 1.2 MHz – a frequency very large compared to that of the disturbance. In large linear colliders, running in a say 1 Hz test mode, this may not be true. Can one use the seismic signals themselves as indicators of their subsequent orbit distortion effects and thereby anticipate and predictably correct between pulses and thus defeat the sampling theorem limitations?

The answer to this seemingly risky question must lie in the degree of *coherence* of the disturbances and some measure of one's ability to sense, compute and correct rapidly. I will take a *cop out* at this point by leaving the pondering of this question as an exercise for the student. To the best of my knowledge this concept has not yet been applied in a physical situation.

Fortunately, in the case of SLC, the inability to deal with transient events is not so serious since these events do *not* occur frequently enough to substantially degrade the average performance of the machine because the particles of the beam are thrown away after each collision and a fresh pulse is generated after each cycle.

In a circular machine *with* damping, a new equilibrium beam size will be established either temporarily or in the steady state depending on the relationship between damping rates and the rates at which disturbances occur.

8. SUMMARY

In the past hour I have meant to introduce you to a subject that has not, up to now, played a major role in accelerator design. The presentation has been fragmented in order to touch on as many facets as possible in the limited time. The key to using this melange of reference information is to return to Fig. 3.4. You can start at any step on the diagram and work either up or down the ladder. If you work upward you are trying to characterize or identify the *sources* of the disturbances. If you work down, you are calculating or attempting to mitigate *consequences*. Each step will be a detailed investigation in its own right.

I hope you have noted that the approach is not one of doom and gloom because I believe that common sense provides the solutions to the various potential problems. I would like, however, to leave you with one thought – as they say on the “Hill Street Blues”²⁷ – ‘be *careful* out there’.

9. REFERENCES

1. Parameters taken from SSC Note-10, LBID-810, Nov. 9, 1983, by Max Cornacchia.
2. Private communications from Alex Chao - SLAC, April 1984.
3. Many of the figures were taken from the text "The Evolving Earth," by F. Sawkins, C. Chase, D. Darby and G. Rapp, Macmillan Publishing Co., 1974, and used with permission of the publishers.
4. W. Herrmannsfeldt *et al.*, Applied Optics, Vol. 17, p. 995, June 1968.
5. T. Lauritzen and R. Sah, IEEE Trans. on Nucl. Sci. Vol NS-28, No. 3 p. 2876, 1981, and Fred Linker, SLAC, PEP Technical Note 251, Nov. 4, 1982, and SLC Collider Note CN 129, October 1981.
6. For example, "Earth Strain Measurements with a Laser Interferometer", J. Berger and R. H. Lovberg, Science, Vol. 170, p. 296-303, October 1970.
7. This figure was kindly provided by W.H.K. Lee of the U.S.G.S. in Menlo Park, California.
8. J. N. Brune and J. Oliver, Bull. Seismology Soc. Am. 49, 349 (1953).
9. Franti *et al.*, Bull. Seismology Soc. Am. 113, (1962).
10. This material is from the excellent text "The Fast Fourier Transform", by E. Oran Brigham, Prentice Hall, Inc., Englewood Cliffs, N.J. (1974). Used with permission of the publishers.
11. "Quantitative Seismology," Vol. I, K. Aki and P. Richards, Freeman & Co., 1980.
12. "Fourier Transforms and their Physical Applications", by D. C. Champaney, Academic Press, 1973.
13. "The American Practical Navigator", Vol. 1, by Defense Mapping Agency Hydrographic Center, 1977 edition.
14. "Comparative Spectra of Microseisms and Swell", R. Haubrich, W. Munk and F. Snodgrass, Bull. Seismological Soc. Am. 53, 27-37, 1963.
15. "A Statistical Analysis of the Generation of Microseisms", K. Hasselman, Reviews of Geophysics, Vol. 1, May 1963.
16. "Microseisms: Coastal and Pelagic Sources", R. Haubrich and K. McCamy, Reviews of Geophysics, Vol. 7, August 1969.
17. The most recent works: "The Lower Limits of Seismic Background Noise Levels," L. G. Holcomb, Proceedings of the ALAA Guidance and Control Conference, 1981. "Vertical Seismic Noise at Very Low Frequencies", D. C. Agnew and Jon Berger, Journal of Geophysical Research, Vol. 83, p. 5420, November 1978.

18. This Table is from the Instruction Manual of the Nicolet FFTA Nicolet Scientific Corporation, Northvale, New Jersey.
19. Private Communication, K. Werner to R. Erickson, SLAC Memo, dated March 1, 1984.
20. G. Fischer and K. Werner, SLAC Collider Note CN-267, May 9, 1984.
21. Compilation taken from an excellent text, "Seismic Waves: Radiation, Transmission and Attenuation", J. E. White, McGraw Hill, N.Y. (1965).
22. N. Ewing and F. Press, Bull. Seismological Soc. Am. 44, p.127-147, (1954).
23. A tutorial may be found in the catalog of the "Mason Industries Inc.", 3335 East Pico Blvd., Los Angeles, CA 90023.
24. Catalog of the "Newport Corporation", 18235 Mt. Baldy Circle, Fountain Valley, CA 92708.
25. Numerical Code for Structural Design, for example see: "Structural Analysis Program for Static and Dynamic Response of Linear Systems", SAP IV (Rev., April 1974), K. J. Bathe, E. L. Wilson and F. E. Peterson, College of Engineering, University of California Berkeley.
26. R. O. Hettel, IEEE, Vol. NS-30, No. 4, p. 2228, August 1983.
27. NBC Television Program, Thursday evenings at 10 p.m.
28. T. Aniel and J. L. Laclare, "Sensitivity of the ESRP Machine to Ground Motion," Laboratoire National Saturne, CEN/Saclay, France, LNS/086 (January 2, 1985).